

# Green Hydrogen from Offshore Wind Power Hubs

Alessandro Singlitico, Jacob Østergaard, Spyros Chatzivasileiadis

Center for Electric Power and Energy (CEE), Department of Electrical Engineering, Technical University of Denmark (DTU), 2800 Kgs. Lyngby, Denmark.

Corresponding author: ales@elektro.dtu.dk

## Abstract

Massive investments in offshore wind power generate significant challenges on how this electricity will be integrated in the incumbent energy systems. In this context, green hydrogen produced by offshore wind, emerges as a promising solution to remove barriers towards a carbon-free economy in Europe and beyond. Motivated by the recent developments in Denmark with the decision to construct the first Offshore Energy Hub in the North Sea, this paper investigates how we can achieve the lowest production cost for green hydrogen. Taking a holistic approach, we consider the integrated co-design of the hydrogen and offshore electricity infrastructure, explore the synergies, and determine the levelized costs of both hydrogen and electricity. We investigate alternative electrolyser placements, technologies, and modes of operation. We find that producing hydrogen offshore reduces the levelized cost of electricity and achieves the lowest cost for hydrogen, competitive with the hydrogen costs currently produced by natural gas.

Concrete actions to accelerate the transition to a net-zero greenhouse gas emissions society have been taken across the European Union (EU) and beyond<sup>1</sup>. In February 2021, the Danish Parliament mandated the construction of the first artificial Energy Island in the North Sea as an initial step to harvest the abundant far offshore wind potential<sup>2,3</sup>. This Energy Island<sup>4</sup> will act as a Hub, interconnecting 3 GW of offshore wind power plants (OWPPs) and transmitting the produced electricity to shore, at much lower costs than the conventional radially-connected OWPPs<sup>5</sup> (**Figure 1**).

Only in the EU, the OWPPs capacity is expected to increase from the current 12 GW to 300 GW by 2050, of which 60 GW will be installed by 2030<sup>6,7</sup>. International consortia, including countries surrounding the North Sea, are planning the next steps with the construction and future expansion of such offshore energy Hubs<sup>8,9</sup>.

However, the integration of massive amounts of offshore wind introduces three main challenges. First, the high variability of wind power production places the supply-demand grid balance at risk. Second, the planned offshore installations require grid reinforcements in the order of billions of Euros<sup>5,10</sup>. Third, electricity will still face challenges with penetrating the so-called hard-to-abate sectors (e.g. heavy-duty road transport, aviation, shipping, and the steel industry), for which more energy-dense carriers are required.

Water electrolysis, using green electricity to generate hydrogen (H<sub>2</sub>), is a potential solution to these challenges. Storable for longer periods and in larger quantities than electricity, H<sub>2</sub> can support the supply-demand balance of the grid, help avoid grid reinforcements, and form the basis of green fuels (e.g. methane, ammonia, and methanol)<sup>11</sup>. Acknowledging these benefits, EU members set the ambitious goal to install electrolyzers of 40 GW total capacity in Europe by 2030, and support

the installation of an additional 40 GW in the EU's neighbourhood, to have this imported to the EU<sup>12</sup>.

Considering that the production of green H<sub>2</sub> will be closely associated with the Offshore Energy Hubs, and the central role H<sub>2</sub> is expected to play in the energy economy, one key question arises: how can we achieve the lowest green H<sub>2</sub> production cost?

To answer this question, in this paper, we take a holistic approach: we propose a techno-economic model which considers the integrated co-design of both H<sub>2</sub> and offshore electricity infrastructure; so far, these have been considered only separately<sup>13–16</sup>. Our approach allows us to identify the interactions and potential synergies between the two energy carriers, and determine the levelised cost of H<sub>2</sub> (LCOH) and electricity (LCOE). Our analyses consider, among others, three main parameters. First, the location of the electrolyzers: onshore, offshore or in-turbine. Second, the share of the electricity routed towards H<sub>2</sub> production: “hydrogen-driven”, if priority is given to the electrolyzers, or “electricity-driven”, if only the excess electricity is directed to the electrolyzers. Third, the type of electrolyser technology: alkaline, proton exchange membrane, or solid oxide.

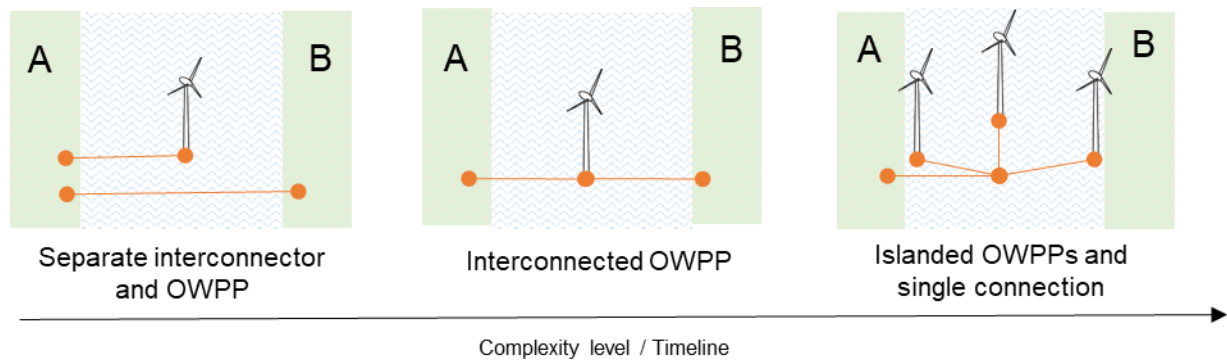


**Figure 1.** Evolution of the offshore power transmission infrastructure<sup>17</sup>. A, B: generic countries.

## Results

### Model Framework

As a reference case for the study, we considered the Hub and Spoke configuration as originally assumed by the North Sea Wind Power Hub Consortium<sup>18,19</sup>: OWPPs with a total capacity of 12 GW connected to an offshore Hub (“Energy Island”) 380 km off the shores of Esbjerg, Denmark.

In our analysis, we investigated three different electrolyser placements (**Figure 2**) along with their related infrastructures:

- I. Onshore: the electricity produced by all OWPPs is collected at the Hub and transmitted to shore, where a single electrolyser is used to produce H<sub>2</sub>, then compressed and delivered to the H<sub>2</sub>-grid.
- II. Offshore: the electricity produced by all OWPPs is transmitted to the Hub, where a single electrolyser, using desalinated seawater, is used to produce H<sub>2</sub>, then compressed and transported to shore via pipelines.
- III. In-turbine: the electrolysers are located inside or next to the tower of each wind turbine (WT), and are paired with desalination units. The produced H<sub>2</sub> is transported to the Hub via smaller pipelines that connect groups of WTs. On the Hub, the H<sub>2</sub> from the OWPPs is collected, compressed, and transported to shore via a larger pipeline.

It is assumed that the cost of the electricity used by the electrolyser is related to the components of the offshore electricity infrastructure upstream of the electrolyser (see Methods).

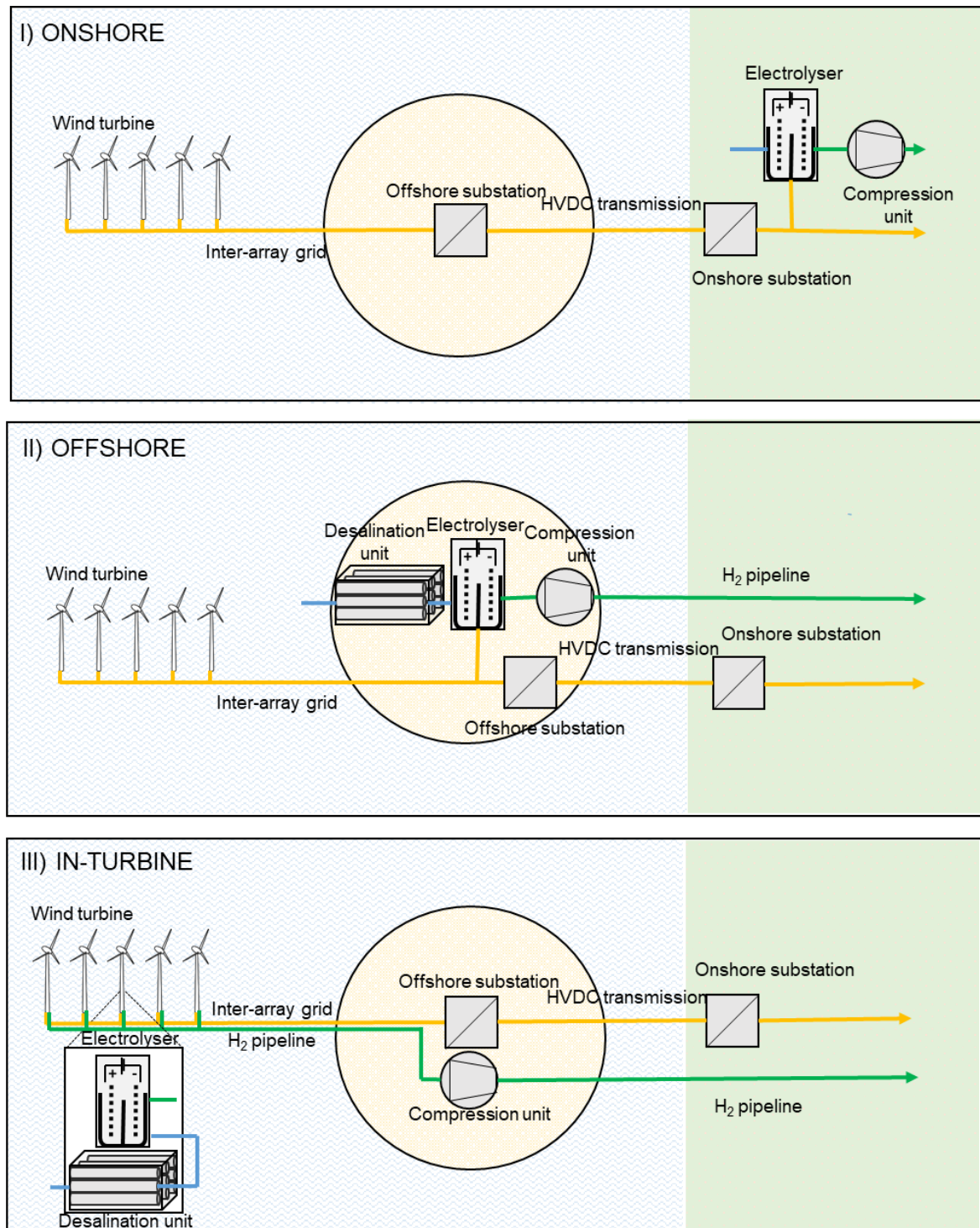


**Figure 2.** Schematic representation of the electrolyser placements.

We assumed two operational modes (illustrated in **Figure 3**) for the cogeneration of electricity and H<sub>2</sub>:

- I. hydrogen-driven: the electricity generated by the Hub is used to cover the nominal electrolyser capacity, and only the remaining electricity is directed to shore. In this case, the electrolyser uses the base load electricity production.
- II. Electricity-driven: the electrolyser consumes only the excess electricity generated. In this case, priority is given to covering the electricity demand, and the electrolyser shaves the peak load.

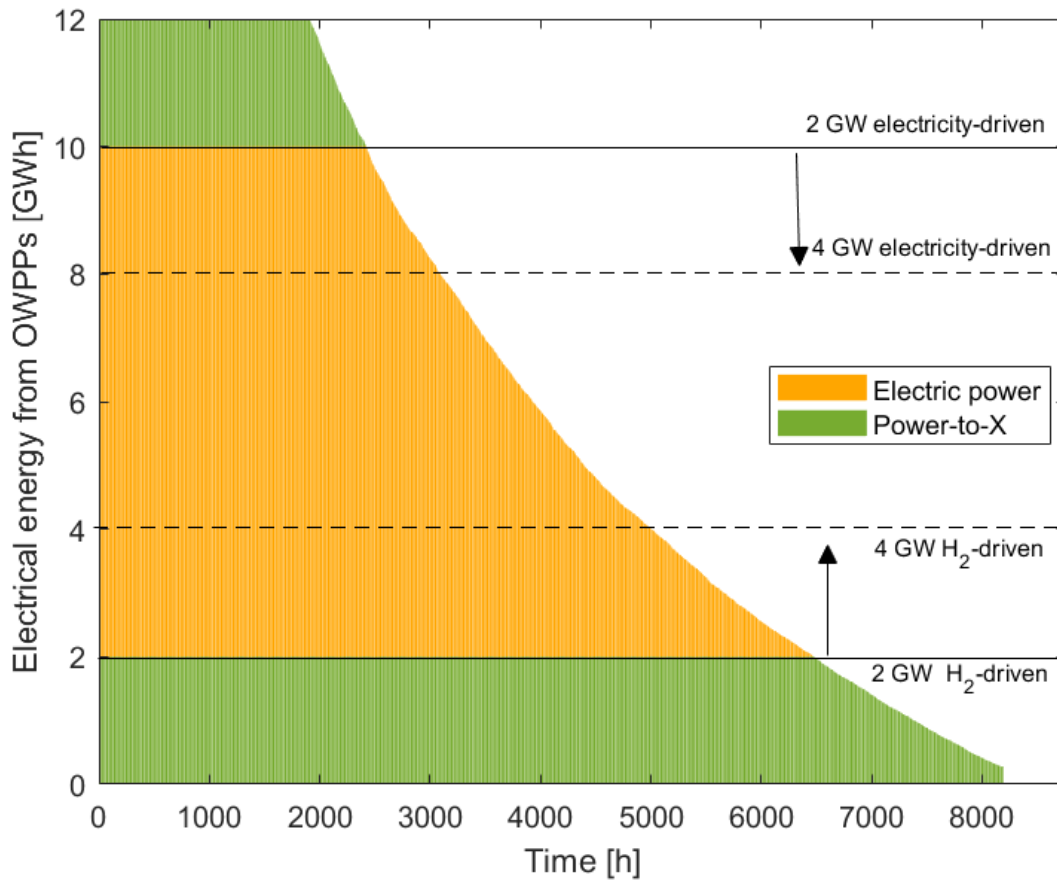


**Figure 3.** 12 GW Hub used by the hydrogen-driven and the electricity-driven operation for a 2 GW electrolyser. Dashed lines show the wind energy for a 4 GW electrolyser.

To appropriately study the impact of the two operation modes, we carried out the analysis through the whole range of possible electricity-H<sub>2</sub> ratios from 100% electricity – 0% H<sub>2</sub> production to 0%

electricity – 100% H<sub>2</sub> production, resizing the electricity and hydrogen infrastructures accordingly in each case.

To properly account for differences in CapEx and operational characteristics, we considered the three main electrolyser technologies<sup>20</sup>: alkaline (AEL), proton exchange membrane (PEMEL) and solid oxide (SOEL).

After we have designed the H<sub>2</sub> and the electricity infrastructure in a complementary and considering the aforementioned electrolyser types, placements and operation modes, the LCOH and LCOE delivered to shore are calculated. The Supplementary Material includes the full mathematical description of the model.

To put the results into context, we compared LCOH with the cost of grey and blue H<sub>2</sub>; grey H<sub>2</sub> is produced from natural gas and costs 0.8-2.7 €/kg<sup>21</sup>; blue H<sub>2</sub> is produced from natural gas as well but it also includes the carbon capture, and costs 1.3-2.4 €/kg<sup>21</sup>. LCOE is compared with the current cost of offshore wind electricity in Europe, which is 45-79 €/MWh<sup>22</sup>.

### **Alkaline Electrolyser is (marginally) more cost-efficient.**

Here we briefly compare the results for the three main electrolyser technologies. As discussed in more detail in the Supplementary Material, AEL presents the lowest LCOH, due to lower CapEx and better overall system performance.

PEMEL achieves higher capacity factors (CFs) mainly due to its lower electric consumption: PEMEL operates at a higher pressure, 55 bar<sup>23</sup>, which limits the use of an external compression unit. This allows a higher share of electricity to be used for H<sub>2</sub> production compared to AEL and SOEL.

Similarly, despite SOEL having the highest efficiency of the three technologies, SOEL's lower operating pressure, 5 bar<sup>20</sup>, requiring more energy for the compression, and the higher degradation rate of its stack<sup>24</sup>, results in higher LCOH compared with AEL.

AEL's lower LCOH compared with PEMEL and SOEL transcends across all operating and placement scenarios in our studies. Therefore, for the sake of readability, we only refer to the results associated with AEL in the next sections.

### **Hydrogen-driven operation achieves cost-competitive green hydrogen production**

Here we present the results for the hydrogen-driven operation (**Figure 4**). Three main factors affect LCOH: the utilisation of the infrastructure, the cost of the electricity supplied to the electrolyser, and the economies of scale for the different components.

The utilisation of the hydrogen or electricity infrastructure can be described by their CF. For the hydrogen-driven operation, the larger the electrolyser installed capacity, the lower its CF (**Figure 3**). The CF is affected in two ways by the placement of the electrolyser. On one side, the lower the electrical consumption of the ancillary-equipment associated with that placement (i.e. desalination and compression units), the more electricity is used by the electrolyser, increasing its CF. On the other side, the more components of the electricity infrastructure are upstream of the electrolyser, the larger are the electrical losses, reducing the CF of the electrolyser.

A second driver for the LCOH is the cost of electricity supplied to the electrolyser. The use (or not) of the inter-array grid and HVDC infrastructure, along with the associated electricity losses, to transport electricity to the electrolyser determines the cost of the electricity used. Therefore, the cost of electricity used by the electrolysers placed onshore is higher than the cost of electricity



used by same-sized electrolyzers placed offshore, not using the offshore HVDC infrastructure, or in-turbine, not even using an inter-array grid infrastructure.

The third driver is associated with the economies of scale related to the electrolyzers and the pipelines. Because of their modularity, the economies of scale of the electrolyser are evident only for sizes lower than 100 MW, becoming highly noticeable for sizes lower than 10 MW<sup>24</sup>. Therefore, in-turbine electrolyzers, having capacities necessarily below the size of the WT (15 MW<sup>18</sup>), are affected more strongly by economies of scale.

In the case of pipelines of the same length, increasing the diameter, the cost per capacity decreases. Therefore, in the case of small scales in-turbine placement, the LCOH is penalised by a large number of pipelines from the OWPPs to the Hub.

As shown in **Figure 4A**, placing the electrolyser on the Hub (i.e. offshore electrolysis) achieves the lowest LCOH, with a minimum of 2.4 €/kg. Irrespective of the installed capacity, offshore electrolysis can produce H<sub>2</sub> at a cost-competitive with the grey H<sub>2</sub>.

**Figure 4B** shows how LCOE varies with different electrolyser placements and installed capacity. In the case of hydrogen-driven operation, as the electrolyser capacity increases, the utilisation of the electricity infrastructure (i.e. *CF-El*) decreases; this results to LCOE increasing when large amounts of H<sub>2</sub> are produced, in case the electrolyser is placed offshore or in-turbine. Besides the lower CF, the main driver for this increase is the fixed costs of HVDC and inter-array cables, which heavily depend on their length and significantly less on their capacity. Moreover, as expected, in case the electrolyser is placed onshore, the LCOE remains unaffected. For the largest part of installed electrolyser capacities, LCOE remains widely competitive with current offshore

wind installations, with the lowest LCOE estimated at 45 €/MWh, in the lower-end of the range of current levelised costs of offshore wind electricity.

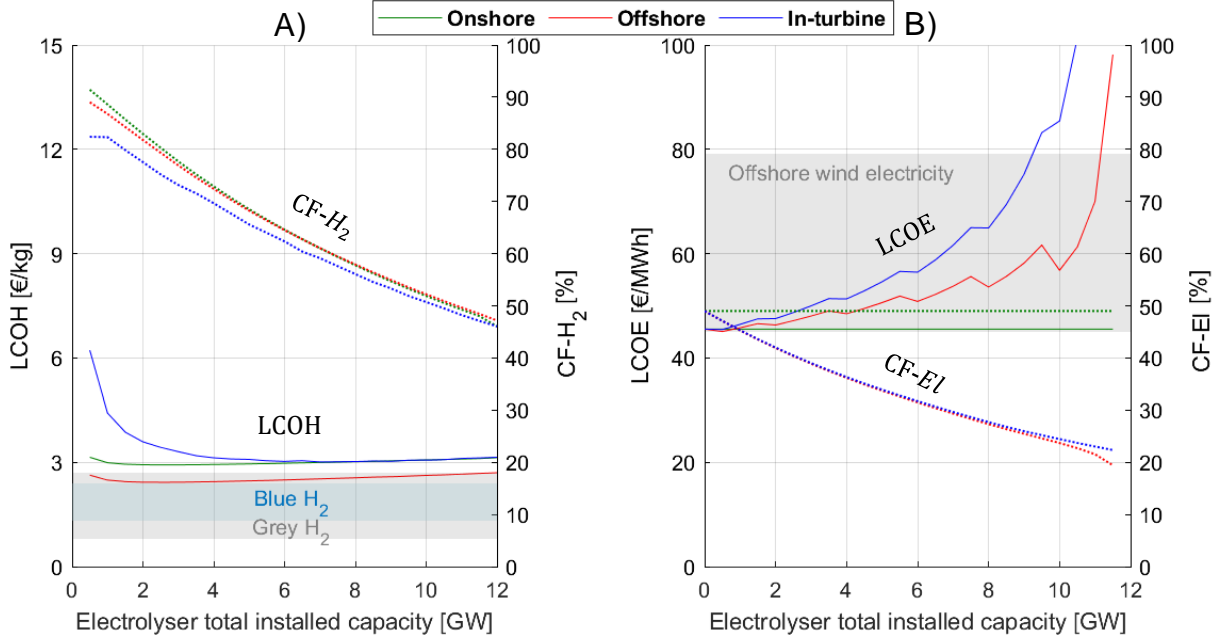


**Figure 4.** LCOH, LCOE and CF for the hydrogen-driven operation. CF- is the capacity factor of the electricity infrastructure (e.g. HVDC transmission cable, HVDC converters, substations, etc.) from the Hub to shore.

### Electricity-driven operation: reduced cost for green electricity

**Figure 5** presents the LCOH and LCOE for the electricity-driven mode of operation. As we reduce the capacity of the electricity infrastructure, and – similar to the hydrogen-driven operation – we increase by an equal amount the installed electrolyser capacity, we observe two effects.

First, the utilisation of the offshore electricity infrastructure will always be higher than that of H<sub>2</sub> ( $CF-El > CF-H_2$ ). As a matter of fact, the lower the electricity infrastructure capacity is (illustrated by a larger electrolyser capacity in **Figure 5**), the higher the CF-El is, and, consequentially the, lower the LCOE will be. The minimum LCOE across all electrolyser placements is 39.4 €/MWh, achieved by offshore electrolysis. Comparing this with the case where no electrolyser is installed

highlights the fact that offshore electrolysis used for peak shaving leads to a 13% reduction of the current cost of offshore wind electricity.

Second, increasing the electrolyser capacity results in an increase in its utilisation (CF- $H_2$  in **Figure 5A**). Therefore, while in the hydrogen-driven operation economies of scale were counteracting the drop in hydrogen infrastructure utilisation, here we have the opposite effect: economies of scale and CF of the electrolyser co-act. As a result, the larger the installed capacity, the lower the LCOH. The lowest LCOH, equal to 2.7 €/kg, is found when all generated electricity is used for full- $H_2$  production.

It is important to remind that in the electricity-driven operation the priority is to cover the electricity demand, therefore the electricity losses of the electrical infrastructure upstream of the electrolyser fully affect utilisation of the electrolyser. This is the reason why small capacities of onshore electrolysers are producing zero hydrogen when the electricity demand is 11.5 GW or higher (i.e. electrolyser capacity of 500 MW).

A final remark about **Figure 5B** related to the LCOE. Beyond electrolyser capacities of 8-10 GW (for a 12 GW offshore Hub), the LCOE starts increasing dramatically, due to the reduced amount of electricity transported compared with the fixed costs of the offshore electricity infrastructure. Therefore, if more than 85% of the offshore wind power is directed towards  $H_2$  production, it might be preferable to have a purely offshore  $H_2$  Hub.

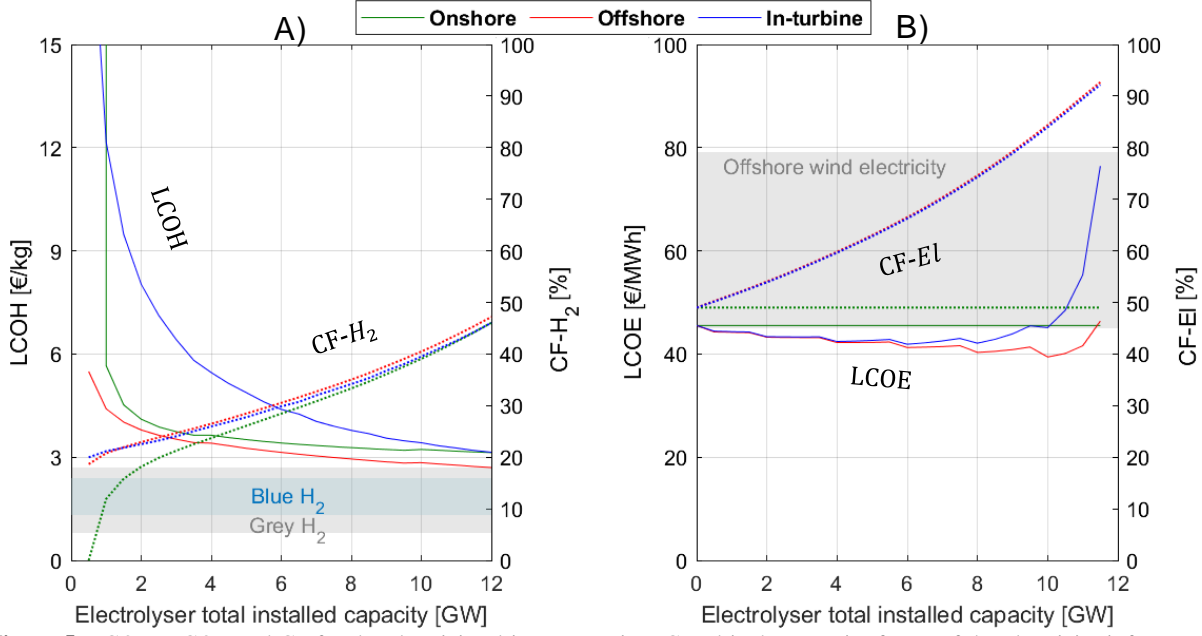


**Figure 5.** LCOH, LCOE and CF for the electricity-driven operation. CF-EI is the capacity factor of the electricity infrastructure (e.g. HVDC transmission cable, HVDC converters, substations, etc.) from the Hub to shore.

### Sensitivity analysis of the component costs

In this section, we examine how the cost of each component affects the median LCOH. We perform a sensitivity analysis by individually changing  $\pm 25\%$  the cost of each component, intending to determine which components have a larger impact on the LCOH. This shall provide insights about which components show the greatest potential for larger H<sub>2</sub> cost reduction.

As shown in **Figure 6**, the cost of the WTs has a major impact, irrespective of the electrolyser placement and operation mode. For hydrogen-driven onshore electrolysis, the HVDC transmission is the second most-relevant component. These results show that the cost of the electrical equipment upstream of the electrolyser is a major component of the LCOH.

Among the hydrogen infrastructure components, the cost of the electrolyser affects the most the median LCOH; this is especially noticeable in the in-turbine placement, where the cost of the electrolyser is penalised by small scales.

Moreover, for the in-turbine placement, we observe that both the pipeline and the compressor costs have a more significant impact compared to the other placements. This happens because, first, several small pipelines need to be installed to transfer the produced  $H_2$  from the OWPPs to the Hub, and second, due to pressure losses in these pipelines, larger compressor capacities are needed on the Hub when compared to the offshore and onshore placements.

It is also very interesting to observe that the costs of the desalination unit and the artificial island have a negligible effect on the LCOH, both in the hydrogen-driven and the electricity-driven operation.

In the case of the electricity-driven operation, the impact of the electrolyser is larger compared to the hydrogen-driven mode. This is because, at a parity of installed capacity (and CapEx), having a lower CF compared to the hydrogen-driven operation, the electrolyser produces less  $H_2$ , thus resulting in a higher cost per unit of kilogram of  $H_2$  delivered. Therefore, a change in the cost of the electrolyser, and the  $H_2$  pipelines, affects more heavily the LCOH.

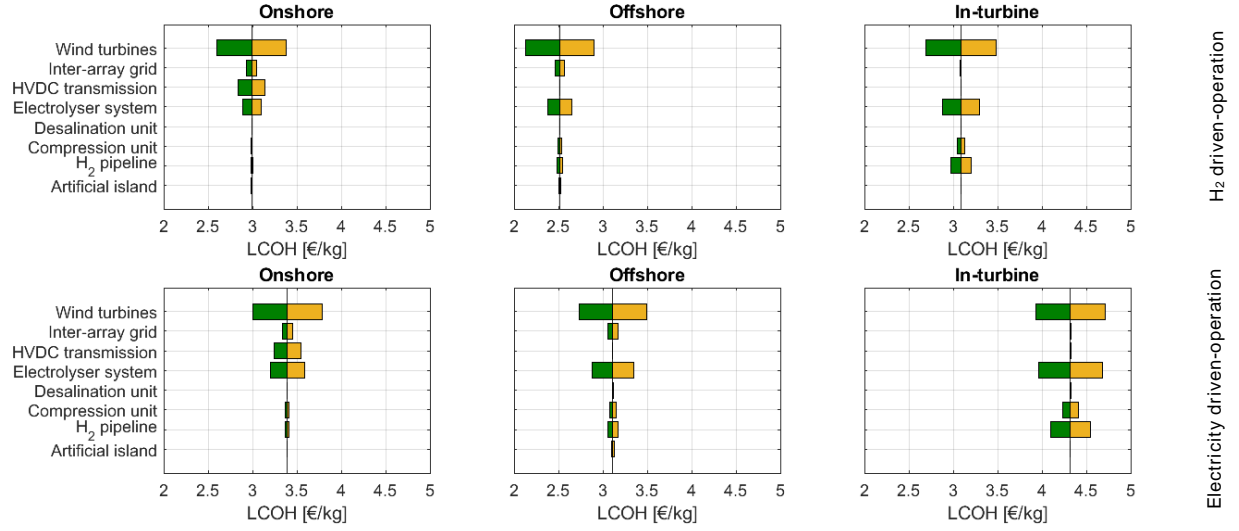


**Figure 6.** Median LCOH obtained by a perturbation of  $\pm 25\%$  of the CapEx of each component. Median LCOH: the median of the LCOHs calculated considering 0.5 GW to 12 GW electrolyser installed capacities

### Impact of distance from shore

Since the exact location of the first Hub is still uncertain and several Hubs are expected to be constructed in the North Sea, in this section, we investigate how the distance of the Hub from shore affects the median LCOH.

As shown in **Figure 7**, there is a slight increase of the median LCOH with increasing distances, but the changes are mild. Offshore electrolysis maintains the lowest median LCOH across the range of possible distances, while in-turbine electrolysis maintains the highest.

It can be observed that the onshore electrolysis curve is steeper than the other two curves; this happens because, for onshore electrolysis, the HVDC transmission plays a major role in determining the LCOH (**Figure 6**). It is possible to conclude that the cost of HVDC lines is more sensitive to distance compared with the H<sub>2</sub> pipelines, used for offshore and in-turbine electrolysis.

Therefore, as the LCOH for in-turbine and offshore electrolysis is only marginally affected by the distance from shore, even more distant applications (i.e. far-offshore) would be possible.

It is also interesting to observe that in the case of hydrogen-driven operation, for shorter distances also the H<sub>2</sub> produced with onshore electrolysis is competitive with grey H<sub>2</sub>.

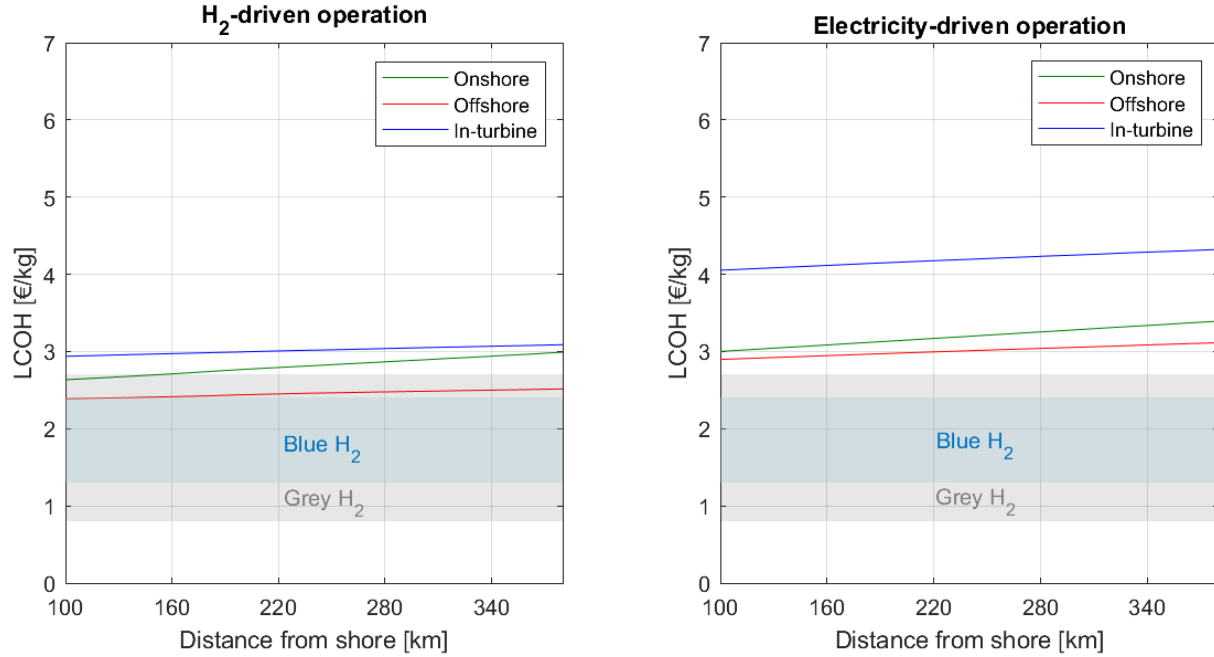


**Figure 7.** Median LCOH per distance of the Hub to shore.

## Conclusions

The holistic techno-economic assessment proposed in this study assessed the cost of production of H<sub>2</sub> and electricity from offshore wind power in the North Sea, comparing three different electrolyser placements (in-turbine, offshore and onshore), three technologies (alkaline, proton-exchange membrane and solid-oxide electrolyzers), and two modes of electrolyser operation (hydrogen-driven and electricity-driven). Results showed that the different types of electrolyzers are equally competitive, with the alkaline electrolyser achieving marginally lower costs. In terms of electrolyser placement, offshore electrolysis resulted in the lowest cost of H<sub>2</sub>. The minimum

LCOH, obtained for offshore electrolysis and hydrogen-driven operation mode, was estimated at 2.4 €/kg, which is competitive with the current costs of grey and blue H<sub>2</sub>.

In the case of the electricity-driven operation of the electrolyser, the cost of electricity reduced up to 13% when compared to the LCOE without any electrolyser installed.

Offshore electrolysis is still not mature in terms of required infrastructure and integration with the offshore power systems, in particular for GW-scale electrolysis. Therefore, the input values for the hydrogen infrastructure have to be considered as estimations determined after discussion with manufacturers and operators. Only the major components of the systems are considered, to limit the complexity of the model and to generate results that would drive more in-depth studies. Moreover, social and environmental analyses were out of the scope. However, these aspects are also necessary to evaluate the feasibility of the placement.

Taking the presented results as a starting point, the cost of offshore green H<sub>2</sub> can further reduce if the hydrogen infrastructure is more tightly integrated with:

- the existing oil and gas infrastructure: e.g. repurposing platforms and pipelines of existing infrastructures.
- the offshore electricity infrastructure: e.g. combining the transmission of H<sub>2</sub> and electricity in a single component, instead of having separate cables and pipelines, and, thus, avoid double installation costs; providing services to the electrical grid, such as a flexible resource for grid balancing.
- the energy/industrial systems: e.g. benefitting from the synergies obtained by using by-products of electrolysis, such as oxygen and heat, and/or further converting H<sub>2</sub> into e-fuels.



## **Methods**

Here we briefly describe the concept of the model used. The extended description is provided in the Supplementary Material.

### **Energy system model**

We assumed a 12 GW scale Hub in the North Sea that can be either deliver electricity or H<sub>2</sub>. So that, the electricity can be alternatively delivered onshore or consumed by an electrolyser to generate H<sub>2</sub>. The main components composing the systems are wind turbines, inter-array grid, HVDC transmission, offshore and offshore substations, electrolyser, compression unit, desalination unit, H<sub>2</sub> pipeline. The electrolyser is assumed to be located either in-turbine, on a centralised offshore Hub or onshore. The system is also investigated at different ratios of electricity/H<sub>2</sub> output from only-electricity (no electrolyser deployed) to only-hydrogen generation. The energy system is investigated as a whole. The placement of the electrolyser determines the equipment used in the infrastructure and the size of the electrolyser determines the size of the equipment deployed for both the H<sub>2</sub> e and the electricity infrastructure. The utilisation of peak or baseload electricity, for the electricity-driven and the hydrogen-driven operations respectively, determine the utilisation of the components, calculated as the capacity factor. Energy and mass balances between the units involved are calculated so that energy losses and efficiencies are accounted for.

For the electrolyser, the main operational parameters are included to evaluate the difference between the different types (alkaline, proton-exchange membranes and solid-oxide electrolyser) in a 2030 perspective: load range, cold start-up time, efficiencies, stack degradation rate, stack lifetime, operating pressure. This is meant to obtain a comparison between the main electrolyser technologies available.

The energy system model is used to calculate the size of each unit, the energy consumption in the system, and the energy delivered onshore in form of electricity or H<sub>2</sub>.

### **Techno-economic model**

Size of the components, energy consumption in the system and energy delivered onshore are then used as input in the techno-economic model. In this model, the levelised cost of the electricity (LCOE) and of the H<sub>2</sub> (LCOH) are calculated and used to compare the different portfolio of solutions.

The sizes of the components are used to calculate capital and operational expenditures (CapEx and OpEx) for each technology unit and then sum up to calculate CapEx and OpEx of the whole system. Gigawatt scales costs are given in form of projection to 2030, using as reference the Energinet Technology Catalogue<sup>20</sup> for the electrolyser and scaled accordingly to scale factors sourced from “Innovative large-scale energy storage technologies and Power-to-Gas concepts after optimization”<sup>24</sup>, so that the economies of scale are accounted. The utilisation of the electrolyser, previously calculated, determines the cost of the stack replacement (not included in the fixed OpEx).

The energy consumption of the system determines the variable costs of the system. The system is considered off-grid, so it does not rely on electrical sources external to the Hub. So, the electricity is assumed to be consumed at its cost of production (LCOE) by the components related to the hydrogen infrastructure (i.e. by the electrolyser, compression unit and desalination unit). The LCOE is calculated at different sections of the offshore electricity infrastructure: (i) in-turbine, (ii) offshore and (iii) onshore. Given the definition of LCOE as the ratio between the actualised sum of the costs of the units involved and the energy delivered, The fewer technology units are involved, the lower is the LCOE for the same unit of energy delivered. So that,  $LCOE(i) < LCOE(ii) < LCOE(iii)$ .

Therefore, the placement of the electrolyser determines the cost at which the electricity is used to produce H<sub>2</sub>. This makes the electricity cheaper for the in-turbine placement, followed by the offshore and the onshore placement. Here comes the fundamental trade-off of this investigation, between the cost of the electricity used (lower when the electrolyser is in the proximity of the source, in-turbine) and the cost of the infrastructure needed to deliver the H<sub>2</sub> onshore (lower when the electrolyser is in the proximity of the demand, on-shore). The levelised cost of the H<sub>2</sub> is finally calculated.

### **Data availability**

The data used in this study are referenced in the main body of the paper and the Supplementary Information. Data that generated the plots in the paper are provided in the Supplementary Information. Additional data and information are available from the corresponding author upon reasonable request.

## References

1. European Commission. *The European Green Deal*. European Commission, Brussels Belgium (2019). doi:10.1017/CBO9781107415324.004
2. Folketinget. *Klimaaftale for energi og industri mv. 2020*. (2020).
3. IRENA. *Hydrogen : a Renewable Energy Perspective*. International Renewable Energy Agency, Abu Dhabi (2019).
4. Energistyrelsen. *Cost benefit analyse og klimaaftryk af energiøer i Nordsøen og Østersøen* *Cost benefit analyse og klimaaftryk af energiøer i Nordsøen og Østersøen*. (2021).
5. North Sea Wind Power Hub Consortium. *Concept Paper 4: Towards Spatial Planning of North Sea Offshore Wind*. (2019).
6. The European Parliament and the Council of the European Union. *Offshore Wind Energy in Europe*. Brussels, Belgium (2020).
7. European Commission. *An EU Strategy to harness the potential of offshore renewable energy for a climate neutral future*. (2020).
8. North Sea Wind Power Hub Consortium. *Modular Hub-and-Spoke Concept to Facilitate Large Scale Offshore Wind*. (2019).
9. Weichenhain, U., Elsen, S., Zorn, T. & Kern, S. *Hybrid projects : How to reduce costs and space of offshore developments North Seas Offshore Energy Clusters study*. (2019).
10. North Sea Wind Power Hub Consortium. *Concept Paper 3: Modular Hub-and-Spoke:*

- Specific solution options.* (2019).
11. Energinet. *Winds of Change In A Hydrogen Perspective - PtX Strategic Action Plan.* (2019).
  12. European Commission. *The hydrogen strategy for a climate-neutral Europe.* (2020).
  13. Meier, K. Hydrogen production with sea water electrolysis using Norwegian offshore wind energy potentials: Techno-economic assessment for an offshore-based hydrogen production approach with state-of-the-art technology. *Int. J. Energy Environ. Eng.* **5**, 1–12 (2014).
  14. Jepma, C. & Van Schot, M. *On the economics of offshore energy conversion: smart combinations\_Converting offshore wind energy into green hydrogen on existing oil and gas platforms in the North Sea.* Energy Delta Institute (2017).
  15. Jepma, C., Kok, G.-J., Renz, M., van Schot, M. & Wouters, K. *North Sea Energy D3.6 Towards sustainable energy production on the North Sea-Green hydrogen production and CO2 storage: onshore or offshore?* (2018).
  16. Crivellari, A. & Cozzani, V. Offshore renewable energy exploitation strategies in remote areas by power-to-gas and power-to-liquid conversion. *Int. J. Hydrogen Energy* **45**, 2936–2953 (2020).
  17. Ørsted. *A European Green Deal - How offshore wind can help decarbonise Europe.* (2019).
  18. E.C.M. Ruijgrok PhD, E.J. van Druten MSc, B. H. B. Ms. *Cost Evaluation of North Sea Offshore Wind Post 2030.* (2019). doi:112522/19-001.830 112522
  19. Swamy, S. K., Saraswati, N., Warnaar, P., Sea, N. & Power, W. *North Sea Wind Power Hub ( NSWPH ): Benefit study for ( 1 + 3 ) potential locations of an offshore hub- island ( Compressed Results ).* (2019). doi:06.37770

20. Danish Energy Agency and Energinet. *Technology Data for Renewable Fuels - Technology descriptions and projections for long-term energy system planning*. (2017).
21. International Energy Agency. Hydrogen production costs by production source. (2020). Available at: <https://www.iea.org/data-and-statistics/charts/hydrogen-production-costs-by-production-source-2018>. (Accessed: 14th March 2021)
22. European Commission. *Report from the commission to the European Parliament and the Council on progress of clean energy competitiveness. Clean Energy Transition - Technologies and Innovations* (2020).
23. IEA. The Future of Hydrogen - Seizing today's opportunities. *Rep. Prep. by IEA G20, Japan* (2019). doi:10.1787/1e0514c4-en
24. Zauner, A., Böhm, H., Rosenfeld, D. C. & Tichler, R. Innovative large-scale energy storage technologies and Power-to-Gas concepts after optimization. D7.7 Analysis on future technology options and on techno-economic optimization. 1–89 (2019).

## **Acknowledgement**

This research has been supported by the North Sea Pre-Feasibility Study project, funded by Det Energiteknologiske Udviklings- og Demonstrations Program (EUDP) under J.nr. 64018-058. The authors also would like to thank the Advisory Board Meeting members.

**Supplementary material**

## **Green Hydrogen from Offshore Wind Power Hubs**

Alessandro Singlitico, Jacob Østergaard, Spyros Chatzivasileiadis

Center for Electric Power and Energy (CEE), Department of Electrical Engineering, Technical University of Denmark (DTU), 2800 Kgs. Lyngby, Denmark.

Corresponding author: [alesi@elektro.dtu.dk](mailto:alesi@elektro.dtu.dk)

## Abbreviations

AC	Alternate current
AEL	Alkaline electrolyser
DC	Direct current
H <sub>2</sub>	Hydrogen
HVDC	High voltage direct current
OWPP	Offshore wind power plant
PEMEL	Proton exchange membrane electrolyser
SOEL	Solid oxide electrolyser
VSC	Voltage source converter

## Symbols

<i>A</i>	Area, m <sup>2</sup>
<i>CapEx</i>	Capital expenditures, M€
<i>CF</i>	Capacity factor, %
<i>CS</i>	Cold start time, min
<i>D</i>	Diameter, mm
<i>DR</i>	Discount rate, %
<i>e</i>	Specific energy, kWh/m <sup>3</sup>
<i>E</i>	Energy, GWh
<i>f</i>	Footprint, m <sup>2</sup>
<i>L</i>	Length, km
<i>LCOE</i>	Levelised cost of electricity, €/kW
<i>LCOH</i>	Levelised cost of H <sub>2</sub> , €/kg
<i>LT</i>	Life time, -
<i>OpEx</i>	Operational expenditures, M€/a
<i>OH</i>	Operating hours, h
<i>N</i>	Number, -
<i><math>\dot{m}</math></i>	Mass flow rate, kg/h
<i><math>\tilde{m}</math></i>	Molar mass, kmol/kg
<i>M</i>	Annual mass, kg/a

$\bar{P}$	Nominal power, GW
$P$	Power, GW
$p$	Pressure, bar
$R$	Ideal gas universal constant, kJ/kg/K
$RC$	Reference cost, -
$RP$	Reference power, MW
$RU$	Reference unit, -
$SF$	Scale factor, -
$t$	Time, h
$W$	Water consumption, l/kg
$T$	Temperature, K
$\dot{V}$	Volumetric flowrate, m <sup>3</sup> /h
$V$	Volume, m <sup>3</sup>
$\varepsilon$	Power load, %
$\eta$	Efficiency, %

#### **Subscripts and superscripts**

<i>COMP</i>	Compressor
<i>DOWN</i>	Downstream
<i>EQ</i>	Equipment
<i>ELEC</i>	Electrolyser
<i>ELEN</i>	Electrical energy
<i>DES</i>	Desalination unit
<i>H</i>	Hour
<i>HS</i>	Hub-to-shore
<i>HUB</i>	Hub
<i>HYD</i>	Hydrogen
<i>IG</i>	Inter-array grid
<i>IN</i>	Inlet
<i>MAX</i>	Maximum value
<i>MEAN</i>	Mean value
<i>MIN</i>	Minimum value
<i>NEQ</i>	Non-equipment



<i>OUT</i>	Outlet
<i>PIPE</i>	Pipeline
<i>PS</i>	Protected shore
<i>RG</i>	Real gas
<i>S</i>	Section
<i>ST</i>	Station
<i>UP</i>	Upstream
<i>OWPP</i>	Offshore wind power plant
<i>WAT</i>	Water
<i>Y</i>	Year

## 1 Methods and materials

In **Section 1.2**, the relation between the share of the electricity converted into H<sub>2</sub> and the share of the electricity delivered to shore is defined, characterising the operations of the electrolyser. In **Section 1.3**, the units of the equipment involved in the electrical and H<sub>2</sub> infrastructures are modelled, calculating the mass and energy balances between them, defining their sizes. In **Section 1.4**, the techno-economic assessment is carried out. The result provides the levelised cost of the H<sub>2</sub> (LCOH) and the levelised cost of the electricity (LCOE) delivered onshore. These economic parameters are used to compare alternative scenarios, obtained by the combination of two types of operation modes, three electrolyser technologies, and three placements. The model is built in Matlab 2019b <sup>1</sup> and Cantera 2.4 <sup>2</sup>.

### 1.1 Input values summary

#### Thermodynamic values

LHV <sub>HYD</sub>	33.33 kWh/kg
T <sub>MEAN</sub>	285.15 K
T <sub>BASE</sub>	288.15 K
p <sub>BASE</sub>	101,325 Pa
G <sub>HYD</sub>	0.0696 [-]
R	8.31434 J/mol K
T <sub>C</sub>	33.2 K
p <sub>c</sub>	1,320 kPa
$\mu$	8.64 10 <sup>-5</sup> poise

#### Technological values

$P_{WT}$	15 MW	3
$N_{WT}$	5	4
$SP_{WT}$	4.5 MW/km <sup>2</sup>	5
$\eta_{IG}$	0.55 %	6
$\eta_{HS}$	0.0035 %	7
$\eta_{ST}$	1 %	7
$W_{DES}$	15 l/kg	8
$e_{DES}$	3.5 kWh/m <sup>3</sup>	9
$\eta_{COMP}$	50%	8
$\varepsilon$	0.05 mm	10
$f_{HVDC}$	4'860 m <sup>2</sup> /GW	11
$h$	33 m	4
$L_{HS}$	380 km	12
$P_{HUB}$	12 GW	4
$P_{OWPP}$	1 GW	4
$p_{TRANS}$	70 bar	13
<b>Economic values</b>		
$DR$	5%	13
$LT$	30 years	4

The Hub and Spoke (H&S) configuration is a recently explored grid connection system. This envisions the deployment of an offshore Hub, where electricity from surrounding offshore wind power plants (OWPPs) is converted to DC, and then transported to shore via high voltage direct current (HVDC). For far OWPPs, the H&S concept has been found more cost-efficient than the radial HVDC connections to individual wind OWPPs, benefiting from the economies of scale of collecting a large amount of power <sup>4</sup>. This study proposes a reference case of a 12 GW Hub, as assumed by the North Sea Power Hub Consortium's work<sup>4</sup>, located 380 km from Esbjerg (Denmark) <sup>12</sup> (**Figure 1**).



**Figure 1.** Original Hub position in the North Sea <sup>12</sup>.

## 1.2 Electrolyser operation modes

In this section, the two main operation modes of the electrolyser concerning the electricity consumed from the OWPPs are described. Considering the cogeneration of electricity and  $H_2$  in the Hub, is it possible to have  $H_2$ -driven or electricity-driven operation modes.

- I.  $H_2$ -driven: the electricity generated by the Hub covers the electrolyser nominal capacity, and only the excess electricity is directed onshore. Therefore, the electrolyser consumes the electrical baseload production of the Hub.
- II. Electricity-driven: the electrolyser consumes the excess electricity from the Hub, namely the peakload production of the Hub.

The electrical energy directed to  $H_2$  production at any hour  $t$ ,  $E_{PtX}(t)$  is calculated using Eq. (1).

$$E_{PtX}(t) = \begin{cases} \min(\bar{P}_{ELEC} \cdot \Delta t, E_{HUB}(t)), & \text{if } H_2 - \text{driven} \\ E_{HUB}(t) - \min(\bar{P}_{HUB} \cdot \Delta t - \bar{P}_{ELEC} \cdot \Delta t, E_{HUB}(t)), & \text{if electricity - driven} \end{cases} \quad (1)$$

where  $E_{HUB}(t)$  is the electricity generated by the Hub at the time  $t$ ; and  $\bar{P}_{ELEC}$  is the nominal capacity of the installed electrolyser (example shown in **Figure 2**).

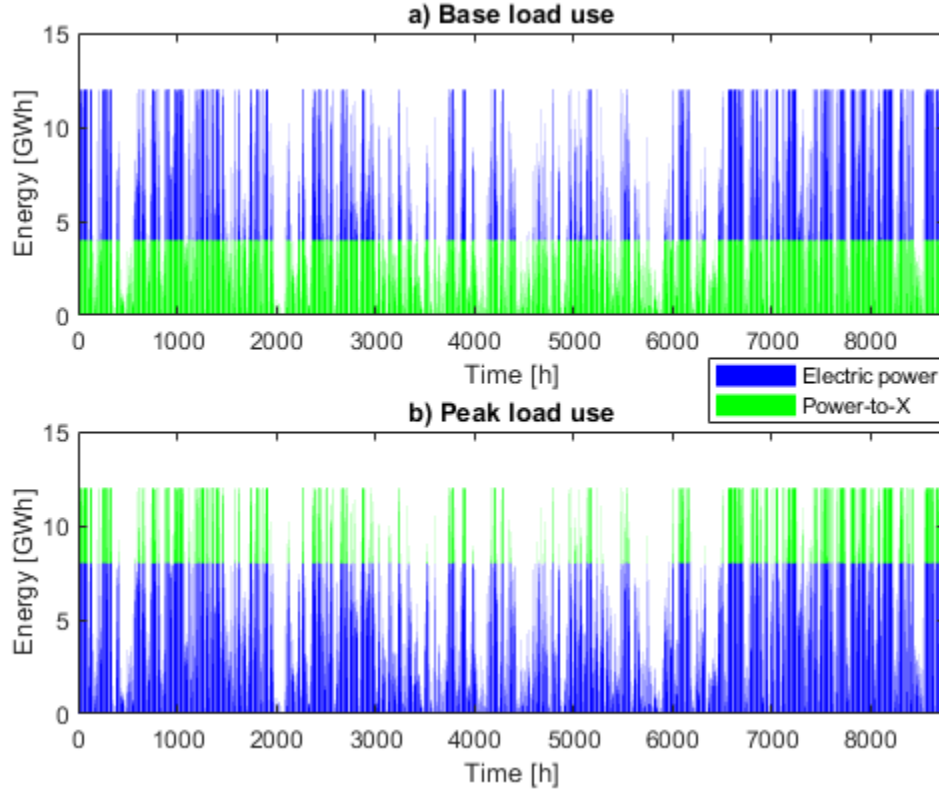


**Figure 2.** The representative annual wind power profile of a 12 GW wind power plant in the North Sea, and use of power for H<sub>2</sub> production through a 4 GW electrolyser, in case of the base (a) and peak (b) load use.

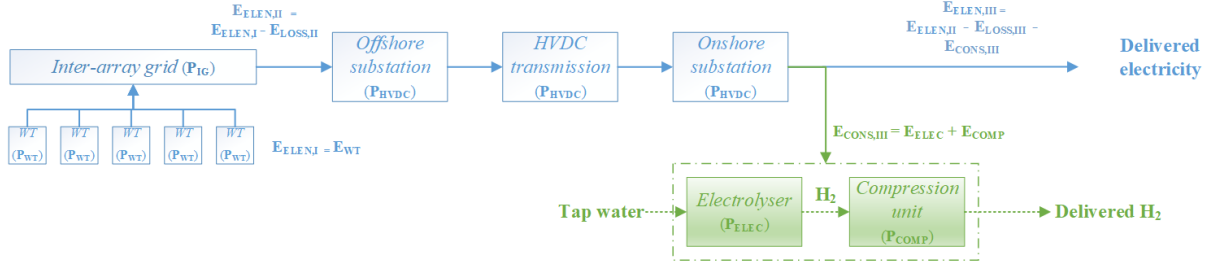
### 1.3 Process design model

Each component is described in this section. Energy,  $E$ , and power,  $P$ , are expressed in units of gigawatt-hours and gigawatt, respectively. **Figure 3** shows the flowchart of the configurations: (i) onshore, (ii) offshore and (iii) in-turbine. The placement of the electrolyser determines the section of the offshore power system at which the electricity is consumed (identified by the subscripts  $I$ ,  $II$ ,  $III$ ). The sum of the electric energy diverted to H<sub>2</sub> production ( $E_{PtX}$ ) is then equal to the sum of the electricity consumption of the electrolyser, desalination unit, and compressor ( $E_{ELEC}$ ,  $E_{DES}$  and  $E_{COMP}$  respectively), as described by Eq. (2).

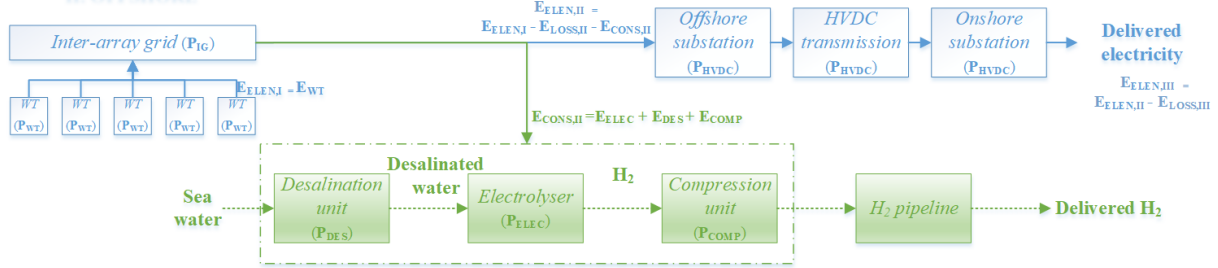
$$E_{PtX}(t) = E_{ELEC}(t) + E_{DES}(t) + E_{COMP}(t) \quad (2)$$

Each component is described in the following subsections.

### I. ONSHORE



### II. OFFSHORE



### III. IN-TURBINE

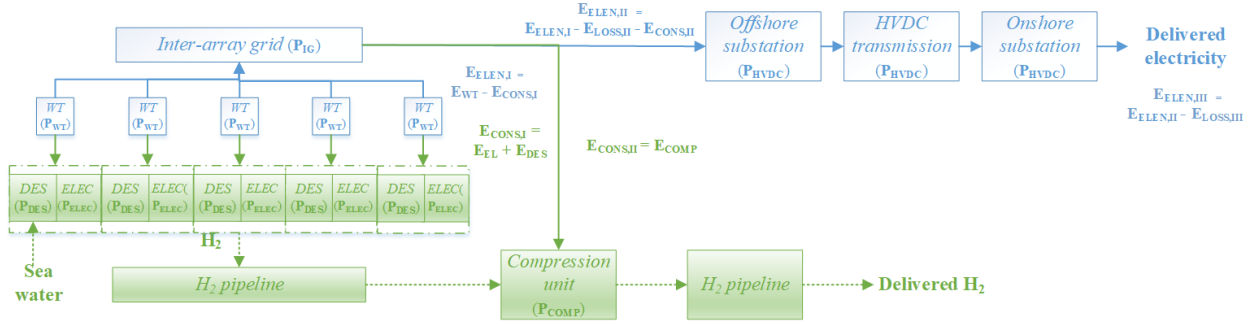


**Figure 3.** Schematic flowchart of the three alternatives. Notes: only one group of WTs connected to the inter-array grid is represented,  $E_{EL,I}$  represents the sum of the energy from each WT. WT: wind turbine; DE: desalination unit; EL: electrolyser.

The Hub is assumed to be composed of wind turbines (WTs) of capacity 15 MW,  $P_{WT}$ . A representative hourly wind power yield, for the position shown in **Figure 1**, is generated from the hourly wind speed data from the Copernicus ERA5 Dataset<sup>14</sup> and considering the International Energy Agency's specifications for a reference 15 MW turbine<sup>3</sup>.

In the in-turbine electrolyser configuration, the energy from each WT,  $E_{WT}(t)$ , is consumed for H<sub>2</sub> production,  $E_{CONS,I}(t)$  or transmitted as electricity,  $E_{ELEN,I}(t)$ , as described in Eq. (3).

$$E_{ELEN,I}(t) = E_{WT}(t) - E_{CONS,I}(t) \quad (3)$$

#### 1.3.1 Inter-array grid

The Hub is assumed to be constituted by a series of concentrically distributed OWPPs of 1 GW of power capacity, as shown in **Figure 4**. Each group of 5 WT,  $N_{WT}$ , is then connected to the Hub through 66 kV AC cables<sup>4</sup>. The length of each string,  $L_{IG}$ , is calculated as the sum of the distance between each WT,  $L_{WT}$ , and the average distance of each OWPP to the Hub,  $L_{HUB}$ , using Eq. (4)

$$L_{IG} = L_{WT} \cdot (N_{WT} - 1) + L_{HUB} \quad (4)$$

The distance between each WT,  $L_{WT}$ , is calculated using Eq. (5)

$$L_{WT} = \sqrt[2]{\frac{P_{WT}}{PY_{WT}}} \quad (5)$$

where  $PY_{WT}$  is the power yield of the WT, assumed 4.5 MW/km<sup>2.5</sup>.

The average distance of each  $n$  OWPP from the Hub,  $L_{HUB}$ , is calculated using Eq. (6).

$$L_{HUB,OWPP(n)} = \frac{1}{2} \cdot \left[ \left[ \frac{n}{4} \right] \cdot \sqrt[2]{\frac{P_{OWPP}}{PY_{WT}}} \cdot \frac{12}{\pi} - \sqrt[2]{\frac{A_{OWPP} \cdot 4}{\pi}} \right] + \left[ \frac{n}{4} \right] \cdot \sqrt[2]{\frac{P_{OWPP}}{PY_{WT}}} \cdot \frac{4}{\pi} \quad (6)$$

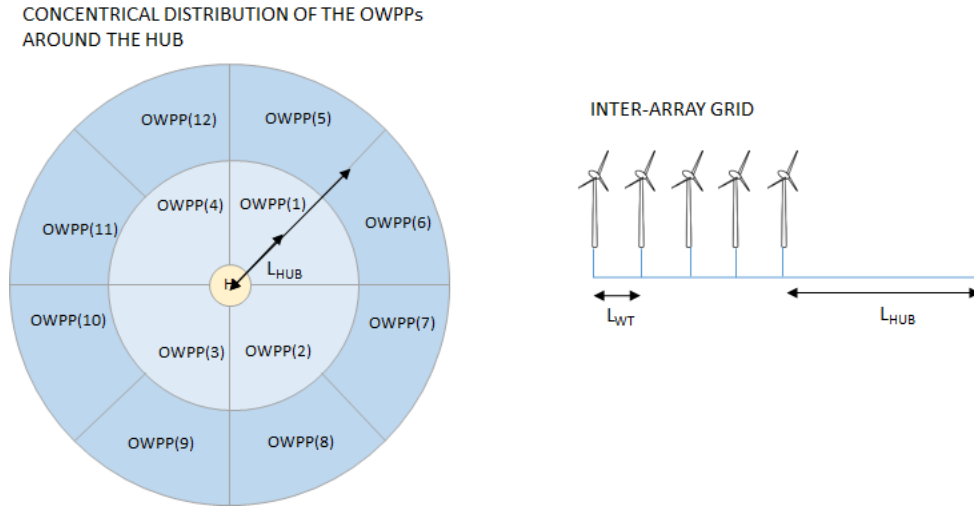


**Figure 4.** Representation of the concentric distribution of each OWPP from the centre of the Hub.

The nominal power of each string,  $\bar{P}_{IG}$ , is calculated using Eq. (7).

$$\bar{P}_{IG} = N_{WT} \cdot \max \left( \frac{E_{ELEN,I}(t)}{\Delta t} \right) \quad (7)$$

The electricity loss from each string to the Hub,  $E_{LOSS,II}(t)$ , is calculated using Eq. (8).

$$E_{LOSS,II}(t) = N_{WT} \cdot E_{ELEN,I}(t) \cdot \eta_{IG} \quad (8)$$

where  $\eta_{IG}$  is the electric energy loss in the inter-array grid, assumed equal to 0.55% of the electric energy transmitted<sup>6</sup>.

The total number of strings,  $N_{IG}$ , is calculated using Eq. (9).

$$N_{IG} = \frac{P_{HUB}}{P_{WT} \cdot N_{WT}} \quad (9)$$

### 1.3.2 HVDC transmission

The electrical energy generated is collected on the Hub, on which the AC is converted into high voltage direct current (HVDC) through voltage source converters. The electric energy transmitted from the Hub onshore,  $E_{ELEN,II}(t)$ , is calculated using Eq. (10).

$$E_{ELEN,II}(t) = N_{IG} \cdot [N_{WT} \cdot E_{ELEN,I}(t) - E_{LOSS,II}(t)] - E_{CONS,II}(t) \quad (10)$$

where  $E_{CONS,II}$  is the energy consumed for H<sub>2</sub> production at the offshore Hub level.

The rated power for the offshore substation, HVDC cable and onshore substation,  $\bar{P}_{HVDC}$ , is calculated using Eq. (11).

$$\bar{P}_{HVDC} = \max(E_{ELEN,II}(t)) \quad (11)$$

The energy loss through the HVDC transmission,  $E_{LOSS,III}$ , is calculated using Eq. (12).

$$E_{LOSS,III}(t) = E_{ELEN,II}(t) \cdot (\eta_{ST} \cdot N_{HVDC,ST} + \eta_{HS} \cdot L_{HS}) \quad (12)$$

where  $\eta_{ST}$  is the energy loss at the conversion station;  $\eta_{HS}$  is the energy loss per km;  $L_{HS}$  is the distance from the hub to the shore. In this case,  $\eta_{ST}$  is assumed to be equal to 1%<sup>7</sup>;  $\eta_{HS}$  is assumed to be 0.0035%<sup>7</sup>;  $L_{HS}$  is estimated to be 380 km from the Hub location to the Denmark shore<sup>12</sup>.

The electricity delivered onshore,  $E_{ELEN,III}(t)$ , is calculated using Eq. (13).

$$E_{ELEN,III}(t) = E_{ELEN,II}(t) - E_{LOSS,III}(t) - E_{CONS,III}(t) \quad (13)$$

where  $E_{CONS,III}(t)$  is the energy consumed for H<sub>2</sub> production onshore.

### 1.3.3 Electrolyser system

The main electrolyser technologies, alkaline (AEL), proton exchange membrane (PEMEL), solid oxide electrolysis cell (SOEL) electrolyzers, are investigated. The operational parameters used in the model are listed in **Table 1**.

**Table 1.** Electrolyser system operational parameters for Alkaline (AEL), Proton Exchange Membrane (PEMEL) and Solid Oxide Electrolyser (SOEL).

	AEL	PEMEL	SOEL	Ref.
Operating pressure, $p_{ELEC}$ [bar]	30	55	5	9 15
Operating temperature, $T_{ELEC}$ [°C]	80	85	675	15
System electrical efficiency*, $\bar{\eta}_{ELEC}$ [%]	66	62	79	15
Stack operating time, $OH_{MAX}$ [h]	82,500	85,000	61,320	16 15
Load range, $\varphi_{MIN}$ - $\varphi_{MAX}$ [% $\bar{P}_{ELEC}$ ]	10-110	0-160	0-100	9 15
Cold start up (after 24h stop), $CS$ [min]	20	5	60	17 15
Degradation, $\eta_{DEG}$ [%/1,000 h]	0.10	0.10	0.50	18
Plant footprint, $f_{ELEC}$ [m <sup>2</sup> /GW]	95,000	48,000	7,000	9 15

\*On lower heating value (LHV) basis; including the energy consumption of the electrolyser stacks, gas water separators, demisters, gas drying, water management, lye system (for AEL), system control, power supply<sup>17</sup>.

The chemical energy of the H<sub>2</sub> produced,  $E_{HYD}(t)$ , is calculated using Eq. (14).

$$E_{HYD}(t) = \begin{cases} E_{ELEC}(t) \cdot \eta_{ELEC}(t) \cdot \left(1 - \frac{CS}{60} \cdot \left(\prod_{i=1}^{24} B(t-i)\right)\right), & \bar{P}_{EL} \cdot \Delta t \cdot \varphi_{MIN} \leq E_{ELEC}(t) < \bar{P}_{ELEC} \cdot \Delta t \\ 0, & E_{ELEC}(t) < \bar{P}_{ELEC} \cdot \Delta t \cdot \varphi_{MIN} \end{cases} \quad (14)$$

where  $\bar{P}_{ELEC}$  is the nominal capacity of the electrolyser;  $\varepsilon_{MIN}$  is the minimum partial capacity of the electrolyser;  $CS$  is the cold start time in units of minute.

$\eta_{EL}$  is the efficiency of the electrolyser. For the first hour of operation,  $t = 1$ , the value of  $\bar{\eta}_{EL}$  is presented in **Table 1**. For the following hours of operation,  $t > 1$ , the efficiency is affected by the degradation of the stack of the cell in the electrolyser and it is calculated using Eq. (15).

$$\eta_{ELEC}(t+1) = \eta_{ELEC}(t) \cdot \left(1 - \frac{\eta_{DEG}}{1,000} \cdot B(t)\right) \quad (15)$$

where  $B(t) = 1$  if  $E_{HYD}(t) > 0$ , or  $B(t) = 0$  otherwise;  $\eta_{DEG}$  is the degradation of the efficiency. The number of operational hours of the electrolyser is calculated using Eq. (16).

$$OH = \sum_{t=1}^{LT_H} B(t) \quad (16)$$

where  $LT_H$  is the lifetime of the electrolyser in hours, in this case equal to 8,760 per year for 30 years. For  $\hat{t} = OH_{MAX}$  the stack is replaced. Consequently, the efficiency of the electrolyser the hour following the replacement,  $\eta_{EL}(\hat{t} + 1)$ , is equivalent to  $\bar{\eta}_{EL}$ , as the initial efficiency is restored.

The capacity factor of the electrolyser,  $CF_{EL}$ , defined as the share of operating hours of the electrolyser during its lifetime, is calculated using Eq. (17).

$$CF_{ELEC} = \frac{\sum_{t=1}^{LT_H} E_{ELEC}(t) \cdot B(t)}{\bar{P}_{ELEC} \cdot \Delta t \cdot LT_H} \quad (17)$$

The  $H_2$  mass flow rate is calculated using Eq. (18), in units of kilogram per hour.

$$\dot{m}_{H_2}(t) = \frac{E_{HYD}(t) \cdot 10^6}{LHV_{HYD}} \quad (18)$$

where  $LHV_{HYD}$  is the lower heating value of the  $H_2$ , equal to 33.3 kWh/kg.

#### 1.3.4 Desalination unit

If offshore or in-turbine, the water for the electrolyser system shall be supplied by a desalination unit. In this analysis, it is assumed that the desalination unit is based on reverse osmosis. The volumetric flow rate of the water is calculated using Eq. (19), in units of cubic meter per hour.

$$\dot{V}_{WAT}(t) = \dot{m}_{HYD}(t) \cdot W_{DES} \cdot 10^{-3} \quad (19)$$

where  $W_{DES}$  is the water consumption for each kilogram of  $H_2$  produced, assumed to be 15 litres of water per kilogram of  $H_2$  <sup>8</sup>. The nominal volumetric flow rate of the desalination unit,  $\bar{V}_{DES}$ , is assumed to be the maximum value of  $\dot{V}_{WAT}(t)$ .



The electric energy consumption of the desalination unit is calculated using Eq. (20).

$$E_{DES}(t) = \dot{V}_{WAT}(t) \cdot e_{DES} \cdot 10^{-6} \quad (20)$$

where  $e_{DES}$  is the energy consumption per cubic meter of water processed, assumed to be 3.5 kWh m<sup>-3</sup><sup>9</sup>.

### 1.3.5 Compression unit

The H<sub>2</sub> produced is compressed into a pipeline. The formula for adiabatic compression<sup>19</sup>, Eq. (21), is used to calculate the required energy,  $E_{COMP}(t)$ .

$$E_{COMP}(t) = \frac{286.76 \cdot \dot{m}_{HYD}(t) \cdot T_{MEAN}}{\eta_{COMP} \cdot G_{HYD} \cdot 3.6 \cdot 10^9} \cdot \left( \frac{\gamma \cdot N_{ST}}{\gamma - 1} \right) \cdot \left[ \left( \frac{p_{COMP,OUT}}{p_{COMP,IN}} \right)^{\frac{\gamma-1}{\gamma \cdot N_{ST}}} - 1 \right] \cdot \Delta t \quad (21)$$

where  $\eta_{COMP}$  is the compression efficiency, assumed to be 50%<sup>8</sup> due to frequent load variations;  $\gamma$  is the ratio between the specific heat capacities for H<sub>2</sub> ( $\gamma = cp/cv$ );  $N_{ST}$  is the number of compression stages, for simplicity assumed as 1.

The three placements of the electrolyser determine the value of  $p_{COMP,IN}$  and  $p_{COMP,OUT}$ :

- I. Onshore:  $p_{COMP,IN} = p_{ELEC}$  (**Table 1**),  $p_{COMP,OUT} = p_{TRANS}$  (70 bar<sup>13</sup>).
- II. Offshore:  $p_{COMP,IN} = p_{ELEC}$  (**Table 1**),  $p_{COMP,OUT} = p_{PIPE,IN}$ .
- III. In-turbine:  $p_{COMP,IN} = p_{PIPE,OUT}$ , as outlet pressure of the pipeline connecting the string of WTs to the Hub,  $p_{COMP,OUT} = p_{PIPE,IN}$ , as the inlet pressure of the pipeline connecting the Hub to shore.

The values of  $p_{PIPE,OUT}$  and  $p_{PIPE,IN}$  are determined in the following subsection.

The nominal power of the compressor,  $\bar{P}_{COMP}$ , is assumed to be the maximum value of  $E_{COMP}(t)$  per hour.

### 1.3.6 H<sub>2</sub> pipeline

The sizes of the pipelines, from the WTs to the Hub and from the Hub to shore, are determined using Eq. (22),<sup>19</sup>

$$\dot{V}_{HYD}(T_b, p_b) = \frac{1.1494}{24} \cdot (10^{-3}) \cdot \left( \frac{T_b}{p_b} \right)^2 \cdot \sqrt{\frac{D^5 \cdot (p_{PIPE,IN}^2 - p_{PIPE,OUT}^2)}{Z_{MEAN} \cdot T_{MEAN} \cdot G_{HYD} \cdot L \cdot \lambda}} \quad (22)$$

where  $\dot{V}_{HYD}(T_b, p_b)$  is the volumetric flowrate of the H<sub>2</sub> at standard conditions ( $T_b = 288.15$  K,  $P_b = 1$  bar<sup>19</sup>), in units of cubic meter per hour;  $p_{PIPE,IN}$  and  $p_{PIPE,OUT}$  are the upstream and downstream pipeline pressures in units of kilopascal;  $G_{HYD}$  is the gas gravity of the H<sub>2</sub>, 0.0696, defined as the molar mass of H<sub>2</sub> divided by the molar mass of air;  $T_{MEAN}$  is the mean temperature in the pipeline, assumed to be 285.15 K<sup>20</sup>;  $Z_{MEAN}$  is the dimensionless compressibility factor;  $\lambda$  is the dimensionless coefficient of friction;  $L$  is the length of the pipeline in units of kilometre;  $D$  is the inner diameter of the pipeline in units of meter.

Pipelines from the OWPPs to the Hub and from the Hub to shore are deployed, having the following values:

- I. For the pipelines from the OWPPS to the Hub:  $L = L_{IG}$ ,  $p_{PIPE,IN} = p_{ELEC}$
- II. For the pipelines from the Hub to shore:  $L = L_{HS}$ ,  $p_{PIPE,OUT} = 70$  bar

The compressibility factor  $Z$  is calculated using Eq. (23).

$$Z_{MEAN} = \frac{\left( \frac{p_{R,IN}}{p_{PIPE,IN}} + \frac{p_{R,OUT}}{p_{PIPE,OUT}} \right)}{2} \quad (23)$$

where  $p_R$  is the pressure of the real gas, in kilopascal, calculated using Eq. (24), considering the inlet and outlet pressures of the pipelines.

$$p_R = \frac{R \cdot T_{MEAN}}{v(T_{MEAN}, p) - b} - \frac{a}{\sqrt{T_{MEAN}} \cdot v(T_{MEAN}, p) \cdot (v(T_{MEAN}, p) + b)} \quad (24)$$

where  $R$  is the universal constant of gas,  $8.31434 \text{ J mol}^{-1} \text{ K}^{-1}$ ;  $v$  is the molar volume of the  $H_2$  in units of  $\text{m}^3/\text{kmol}$ ; and  $a$  and  $b$ : factors of the Redlich-Kwong equations, calculated using Eq. 25 and Eq. (25).

$$a = 0.42748 \cdot \frac{R^2 \cdot T_C^{\frac{5}{2}}}{p_C} \quad (25)$$

$$b = 0.08664 \cdot \frac{R \cdot T_C}{p_C} \quad (26)$$

where  $T_C$  is the critical temperature of  $H_2$  equivalent to  $33.2 \text{ K}$ ;  $p_C$  is the critical pressure of  $H_2$  equivalent to  $1,320 \text{ kPa}$ .

The coefficient of friction factor, or Darcy-Weisbach,  $\lambda$  is calculated by solving the Colebrook-White equation for gas in pipelines in turbulent flows ( $Re > 4000$ ), Eq. (27)

$$\frac{1}{\sqrt[3]{\lambda}} = -2 \cdot \log \left( \frac{K}{3.7} + \frac{2.51}{Re \cdot \sqrt[3]{\lambda}} \right) \quad (27)$$

where  $K$  is the roughness factor in a pipeline, calculated using Eq. (28)

$$K = \frac{\epsilon}{D} \quad (28)$$

where  $\epsilon$  is the equivalent sand roughness, assumed  $0.05 \text{ mm}$ <sup>10</sup>; and  $Re$  is the Reynolds number for the flow in a pipe used for gas pipeline design<sup>19</sup>, calculated using Eq. (29).

$$Re = 0.5134 \cdot \left( \frac{P_b}{T_b} \right) \left( \frac{G_{HYD} \cdot \dot{V}_{H_2,PIPE}(T_b, p_b) \cdot 24}{\mu(T_b, p_b) \cdot D} \right) \quad (29)$$

where  $\mu$  is the dynamic viscosity of  $H_2$  at standard conditions,  $8.64 \cdot 10^{-5}$  poise.

The erosional velocity is calculated,  $u_{MAX}$  in units of meter per second<sup>19</sup>, using Eq. (30)

$$u_{MAX} = 100 \sqrt{\frac{Z \cdot R \cdot T_{MEAN}}{29 \cdot G_{HYD} \cdot P}} \quad (30)$$

Acceptable operational velocity,  $u$ , is assumed to be lower than 50% of the erosional velocity in units of meter per second <sup>19</sup>.

Having a known mass flow rate, the velocity  $u$  is related to the diameter of the pipeline  $D$ , according to Eq. (31).

$$\dot{m}_{H_2}(t) = u \cdot \rho(T, p) \cdot \pi \cdot \frac{D^2}{4} \quad (31)$$

where  $\rho$  is the density in units of kilogram per cubic meters.

For the pipeline from the Hub to the shore, the diameter is calculated using Eq. (31), with  $p = p_{TRANS}$ , and  $\rho(T_{MEAN}, p_{TRANS})$ .  $p_{PIPE,IN}$  is then calculated solving Eq. (22).  $p_{PIPE,IN}$  is then equivalent to  $p_{COMP,OUT}$  and it can be used in Eq. (21).

For the pipelines from the OWPPs to the Hub, diameter,  $D$ , and outlet pressure,  $p_{PIPE,OUT}$ , are found maximising  $u_{PIPE,OUT}$ , considering two constraints:  $u_{PIPE,OUT} < 0.5 \cdot u_{MAX}$  and  $p_b \leq p_{PIPE,OUT} \leq p_{PIPE,IN}$ . The higher the velocity the lower is the diameter, having a fixed mass flow rate, thus reducing the cost.

### 1.3.7 Artificial island

The Hub hosting the offshore equipment is assumed to be a sand island, as this is considered to be more cost-effective than other types of offshore platforms in the case of a large hub in shallow waters <sup>21</sup>. The Hub shall have a surface,  $A_{HUB}$ , able to host the HVDC offshore substation and the electrolyser.  $A_{HUB}$  is calculated using Eq. (32), in units of square metre.

$$A_{HUB} = \bar{P}_{HVDC} \cdot f_{HVDC} + \bar{P}_{ELEC} \cdot f_{ELEC} \quad (32)$$

where  $f_{HVDC}$  is the footprint of the offshore substation, here assumed to be 4'860 m<sup>2</sup> /GW <sup>11</sup>, and  $f_{EL}$  is the footprint of the electrolyser. The volume of the sand used to build the island,  $V_{HUB}$ , and the area of the shoreline assumed to be protected,  $A_{PS}$ , are simplified considering the island has the shape of a truncated cone.

The volume of the hub,  $V_{HUB}$ , is calculated using Eq. (33).

$$V_{HUB} = \frac{1}{3} \cdot s \cdot \pi \cdot (r_{SB}^3 - r_{HUB}^3) \quad (33)$$

where  $r_{HUB}$  is the radius at the surface level, and  $r_{SB}$  is the radius at the seabed level, in units of metre, calculated using Eq. (34) and Eq. (35), respectively.

$$r_{HUB} = \sqrt{\frac{A_{HUB}}{\pi}} \quad (34)$$

$$r_{SB} = r_{HUB} + h/s \quad (35)$$

where  $s$  is the slope of the truncated cone, assumed to be 75%;  $h$  is the depth of the seabed, assumed 30 m<sup>4</sup> to which is added 10% of elevation, to be over the sea level.

Moreover, the area of the shoreline assumed to be protected,  $A_{PS}$ , in units of square meters is calculated, using Eq. (36).

$$A_{PS} = \pi \cdot r_{SB}^2 + \pi \cdot r_{SB} \cdot \sqrt{r_{SB}^2 \cdot (1 + s^2)} - \pi \cdot r_{HUB}^2 - \pi \cdot r_{HUB} \cdot \sqrt{r_{HUB}^2 \cdot (1 + s^2)} \quad (36)$$

#### 1.4 Techno-economic analysis

The levelised cost of the electricity (LCOE) and the levelised cost of the H<sub>2</sub> (LCOH) are used to compare the alternative configurations. The LCOEs of each section of the offshore power systems, in-turbine, offshore, and onshore (section I to III in **Figure 3**), are calculated using Eq. (37)-(39), in units of Euro per megawatt-hour of electricity. LCOH accounts for the capital and operating expenditures (CapEx and Opex) of the units involved in the H<sub>2</sub> production systems, as well as the cost of the electricity consumed at each section of the offshore power system. The LCOH is calculated using Eq. (40), in unit of Euro per kilogram of H<sub>2</sub> produced.

**Table 2.** Levelised cost of the energy equations. Note: LCOE<sub>III</sub> is also the final cost of the electricity delivered onshore.

Symbol	Value	Eq.
$LCOE_I$	$\frac{\sum_{Y=0}^{LT_Y} \frac{CapEx_{ELEN,I,Y} + OpEx_{ELEN,I,Y}}{(1 + DR)^Y}}{\sum_{y=0}^{LT_Y} \frac{N_{WT} \cdot N_{WT} \cdot E_{WT,Y}}{(1 + DR)^Y}}$	(37)
$LCOE_{II}$	$\left[ LCOE_I \cdot \frac{\sum_{Y=0}^{LT_Y} \frac{E_{ELEN,I,Y}}{(1 + DR)^Y}}{\sum_{Y=0}^{LT_Y} \frac{E_{ELEN,I,Y} - E_{LOSS,II}}{(1 + DR)^Y}} \right] + \left[ \frac{\sum_{y=0}^{LT_Y} \frac{CapEx_{ELEN,II,Y} + OpEx_{ELEN,II,Y}}{(1 + DR)^Y}}{\sum_{Y=0}^{LT_Y} \frac{E_{ELEN,II,Y} - E_{LOSS,II}}{(1 + DR)^Y}} \right]$	(38)
$LCOE_{III}$	$\left[ LCOE_{II} \cdot \frac{\sum_{Y=0}^{LT_Y} \frac{E_{ELEN,II,Y}}{(1 + DR)^Y}}{\sum_{Y=0}^{LT_Y} \frac{E_{ELEN,II,Y} - E_{LOSS,III}}{(1 + DR)^Y}} \right] + \left[ \frac{\sum_{Y=0}^{PT_Y} \frac{CapEx_{ELEN,III,Y} + OpEx_{ELEN,III,Y}}{(1 + DR)^Y}}{\sum_{Y=0}^{LT_Y} \frac{E_{ELEN,II,Y} - E_{LOSS,III}}{(1 + DR)^Y}} \right]$	(39)
$LCOH$	$\left[ \sum_{S=I}^{III} LCOE_S \cdot \frac{\sum_{Y=0}^{LT_Y} \frac{E_{CONS,S,Y}}{(1 + DR)^Y}}{\sum_{Y=0}^{LT_Y} \frac{M_{HYD,Y}}{(1 + DR)^Y}} \right] + \left[ \frac{\sum_{Y=0}^{PT_Y} \frac{CapEx_{H_2,Y} + OpEx_{H_2,Y}}{(1 + DR)^Y}}{\sum_{Y=0}^{LT_Y} \frac{M_{HYD,Y}}{(1 + DR)^Y}} \right]$	(40)

$DR$  in Eq. (37)-(40) is the discount rate, which reflects the financial return and the project risk, here assumed to be 5%<sup>13</sup>;  $PT_Y$  is the lifetime of the project as the lifetime of the system, 30 years<sup>4</sup>. The pieces of equipment involved in each infrastructure are presented in the flowchart shown in

**Figure 3.** The total CapEx and OpEx are calculated summing the CapEx and OpEx of each unit deployed in the configurations, using the equations in **Table 3**.

**Table 3.** Cost inventory for the calculation of LCOE and LCOH.

Component	Symbol	Value	Comment	Ref.
<b>Capital expenditures, CapEx [M€]</b>				
Wind power plant	$CapEx_{OWPP,EQ}$	$(14 + 7.55) \cdot N_{WT}$	14 M€ represents the cost of all components of a reference 15 MW; 7.55 M€ represents the costs of the substructure underneath the turbine, determined based on the required mass of the tower, transition piece and monopile foundation for an average depth of 30 m.	4
	$CapEx_{OWPP,NEQ}$	$100 \cdot \bar{P}_{OWPP}$	This equation represents the project development, including all costs up to the start of construction.	4
Inter-array grid	$CapEx_{IG,EQ}$	$\sum_i L_{IG,i} \cdot \left[ 94.94 \cdot 10^{-3} + 86.2 \cdot 10^{-3} \cdot e^{\left( \frac{2.05 \cdot P_{IG}}{10^8} \right)} \right]$	Cost equation of AC cables based on a rated voltage of 66 kV.	22
	$CapEx_{IG,NEQ}$	$\sum_i 0.33 \cdot L_{IG,i}$	Installation costs for offshore inter-array grid cables.	22
Offshore substation	$CapEx_{SS,OFF}$	$117.9 \cdot P_{HVDC} + \left[ \frac{P_{HVDC}}{P_{MAX}} \right] \cdot 45.4$	Curve fitting the average of the cost of an offshore VSC-HVDC. $P_{MAX}$ is considered 2 GW.	23
Onshore substation	$CapEx_{SS,ON}$	$101 \cdot P_{HVDC} + \left[ \frac{P_{HVDC}}{P_{MAX}} \right] \cdot 61.6$	Curve fitting the average of the costs onshore VSC-HVDC substations. $P_{MAX}$ is considered 2 GW.	23
VSC-HVDC transmission	$CapEx_{HVDC}$	$L_{HS} \cdot \left[ 0.6 \cdot \bar{P}_{HVDC} + \left[ \frac{\bar{P}_{HVDC}}{P_{MAX}} \right] \cdot 1.345 \right]$	Curve fitting including HVDC extruded copper 320-400 kV and the installation and the average of 2 single cables; 2 trenches, single-core, 10m apart. $P_{MAX}$ is considered 2 GW.	23
Electrolyser system	$CapEx_{EL}$	$\bar{P}_{ELEC} \cdot RC_{ELEC} \cdot (1 + IF \cdot OS) \cdot \left( \frac{\bar{P}_{ELEC} \cdot 10^3}{RP_{ELEC}} \right)^{SF_{ELEC}}$	Non-equipment costs: land, contingency, contractors, legal fees, construction, engineering, yard improvements, buildings, electrics, piping, instrumentation and installation and grid connection. The cost for the offshore configuration is assumed to be double the onshore costs. (OS =1 if the electrolyser is located in-turbine or offshore, OS =0 if the electrolyser is located onshore, reflecting Siemens estimations).	8,24
Desalination unit	$CapEx_{DES}$	$30.6 \cdot \bar{V}_{DES}$	Reverse osmosis seawater desalinators (Lenntech Reverse Osmosis System) is used as reference technology.	13
Compression unit	$CapEx_{COMP}$	$3,000 \cdot \bar{P}_{COMP}$	Considering a centrifugal compressor with electric drivers, including power lines, transformers, and electronics.	25
H <sub>2</sub> pipeline	$CapEx_{PIPE}$	$1.75 \cdot L_{HS} \cdot [0.314 + 0.574 \cdot 10^3 \cdot (D) + 1.7 \cdot 10^6 \cdot (D)^2]$	Pipeline for H <sub>2</sub> transmission in the North Sea.	13
Artificial island	$CapEx_{HUB}$	$(3.26 \cdot V_{HUB} + 804 \cdot A_{HUB}) \cdot 10^{-6}$	The cost of dredged sand is assumed to be 3.26 €/m <sup>3</sup> and the cost for protecting the shoreline of the island is assumed to be 804 €/m <sup>2</sup> . The cost of the artificial island is assumed to be allocated to the electricity and H <sub>2</sub> generated proportionally to the footprint of their components, HVDC offshore substation for the electricity system, and electrolyser for the H <sub>2</sub>	26

<b>Operation and maintenance expenditures, OpEx [M€/a]</b>					
Wind power park	$OpEx_{OWPP}$	$1.9\% \cdot CapEx_{OWPP,EQ}$	-		5
Inter-array grid	$OpEx_{IG}$	$0.2\% \cdot CapEx_{IG,EQ}$	-		27
HVDC	$OpEx_{HVDC}$	$0.2\% \cdot CapEx_{HVDC}$	$CapEx_{HVDC}$ includes the cost of the substations and the transmission line.		27
Electrolyser system	$OpEx_{ELEC,EQ}$	$CapEx_{ELEC} \cdot (1 - IF \cdot (1 + OS)) \cdot 3.44\% \cdot (\bar{P}_{ELEC} \cdot 10^3)^{-0.155}$	Including material cost for planned and unplanned maintenance, labour cost in central Europe, which all depend on a system scale. Excluding the cost of electricity and the stack replacement, calculated separately. Scaled maximum to $\bar{P}_{ELEC} = 1$ GW.		17
	$OpEx_{ELEC,SR}$	$\bar{P}_{ELEC} \cdot RC_{SR} \cdot \left( \frac{\bar{P}_{ELEC} \cdot 10^3}{RP_{SR}} \right)^{SF_{SR}} \cdot \left[ \frac{OH}{OH_{MAX}} \right]$ $RC_{SR} = RU_{SR} \cdot RC_{ELEC} \cdot (1 - IF) \cdot \left( \frac{RP_{SR}}{RP_{ELEC}} \right)^{SF_{ELEC}}$ $SF_{SR} = 1 - (1 - SF_{SR,0}) \cdot e^{-\frac{P_{ELEC}}{P_{STACK,MAX}}}$	Approximation of stack costs and replacement cost depending on the electrolyser equipment costs. Paid only the year in which the replacement is needed.		8,28
	$OpEx_{ELEC,NEQ}$	$4\% \cdot CapEx_{ELEC} \cdot IF \cdot (1 + OS)$	It covers the other operational expenditure related to the facility level. This includes site management, land rent and taxes, administrative fees (insurance, legal fees...), site maintenance.		8
	$OpEx_{DES}$	$2.5\% \cdot CapEx_{DES}$	Operational expenditure of desalination when assumed part of the electrolyser system.		13
Compressor	$OpEx_{COMP}$	$4\% \cdot CapEx_{COMP}$	Fixed operational and maintenance costs.		29
H <sub>2</sub> pipeline	$OpEx_{PIPE}$	$2\% \cdot CapEx_{PIPE}$	Fixed operational and maintenance costs for both $CapEx_{PIPE,HS}$ and $CapEx_{PIPE,WTH}$ .		13
Tap water	$OpEx_{H_2O}$	$9.23 \cdot (1 - 0.6) \cdot 10^{-6} \cdot \sum_{t=1}^{8760} \dot{V}_{H_2O,DES}(t)$	In the case of offshore electrolysis, water is purchased from the grid. 9.23 € per cubic meter of water is assumed as an average price and a 60% discount for large consumers.		30
Conversions used from the original currencies: USD <sub>2014</sub> =0.752 EUR <sub>2014</sub> , EUR inflation from 2014 to 2017 = 1.81%; EUR inflation from 2010 to 2017 = 9.11%; SEK <sub>2003</sub> to = 0.1096 EUR <sub>2003</sub> , EUR inflation from 2003 to 2017 = 25.33%; GBP <sub>2015</sub> = 1.35 EUR <sub>2015</sub> , EURO inflation from 2015 to 2017 = 1.78%.					

### 1.4.1 Electrolyser economies of scale

Large scale electrolyzers are still under development, so no commercial cost reference exists. However, an investigation conducted by Zauner et al.<sup>18</sup> showed that the effect of economies of scale is more pronounced at lower nominal power levels than at higher levels. This leads to an increased share of stack costs in the overall system for larger electrolysis systems, which reduces the overall effect of the economies of scale. In this study, it is assumed that the scale factor for small units is used to calculate the costs for electrolyzers not larger than 10 MW, while the scale factor for large sizes is used for electrolyzers larger than 10 MW. It is also assumed that no additional economies of scale are accounted for in sizes larger than 100 MW. The average costs for the different technologies for 2030 has been sourced from the Energinet Technology Catalogue<sup>15</sup>. (**Table 4**).

**Table 4.** Coefficients used for CapEx<sub>EL</sub> calculations (sourced from<sup>15,18</sup>).

	Reference cost, $RC_{ELEC}$ [€/kW]	Installation fraction*, IF [% $RC_{ELEC}$ ]	Reference power, $RP_{ELEC}$ [MW]	Scale factor, $SF_{ELEC}$ [<10 MW/>10 MW]
AEL	550	27	10	-0.24/-0.13
PEMEL	600	33	10	-0.21/-0.14
SOEL	600	63	15	-0.25/-0.22

\*Installation costs include: land, contingency, contractors, legal fees, construction, engineering, yard improvements, buildings, electrics, piping, instrumentation and installation and grid connection

The economies of scale of each piece of the equipment composing the electrolyser system (i.e. stack, power electronics, gas conditioning, gas conditioning, balance of plant) are different. Therefore, the cost of the stack would not follow the economies of the entire electrolyser unit. The stack does not show potential for large cost reduction via economies of because of its modular design<sup>18</sup>. The values used in the calculations are listed in **Table 5**.

**Table 5.** Coefficients used for OpEx<sub>EL,SR</sub> calculations (sourced from<sup>18</sup>).

	Reference cost share*, $RU_{SR}$ [%]	Average max size, $\bar{P}_{STACK,MAX}$ [MW]	Average scale factor, $SF_{SR,0}$
AEL	45	4	0.12
PEMEL	41	2	0.11
SOEL	50	1	0.13

\*for a reference power,  $RP_{SR}$ , of 5 MW.

## 1.5 Extended results

An initial overview of the specific CapEx of each unit involved in the H<sub>2</sub> infrastructure is shown in **Figure 5**. AEL presents specific CapEx per unit of capacity installed lower than PEMEL and SOEL.

The economies of scale of the electrolyser are visible in the in-turbine configuration, in which the electrolyser size ranges from 625 kW to 15 MW. In the case of offshore and onshore electrolysis,



the cost per installed capacity of the electrolyser is constant, since over 100 MW the economies of scales are assumed not to affect the unitary cost.

The CapEx of the pipelines for distribution (i.e. from the OWPPS to the Hub) and transmission (i.e. from the Hub to shore) is affected by the number of the pipelines and their diameter. In the in-turbine case, because of the large number of pipelines involved and their small diameters, the CapEx of the distribution pipelines is a substantial share of the cost, especially in the case of small installed capacities, due to economies of scales of the pipeline. The effect of the economies of scales is evident also in the CapEx of the transmission pipeline in the case of offshore electrolysis.

The CapEx of the compressor is affected by its pressure ratio ( $p_{OUT}/p_{IN}$ ): the larger the pressure ratio, the larger the CapEx of the compressor. The operating pressure of the electrolyser and the placement of the electrolyser affect the pressure ratio of the compressor. Higher operating pressure of the electrolyser results in a lower additional compression. Moreover, the closer to shore is the placement, the lower is the pressure ratio, since fewer are the pressure losses (i.e. in the pipelines from the OWPPs to the Hub and from the Hub to shore). The CapEx of the artificial island and the desalination unit have a minor share on the overall CapEx.

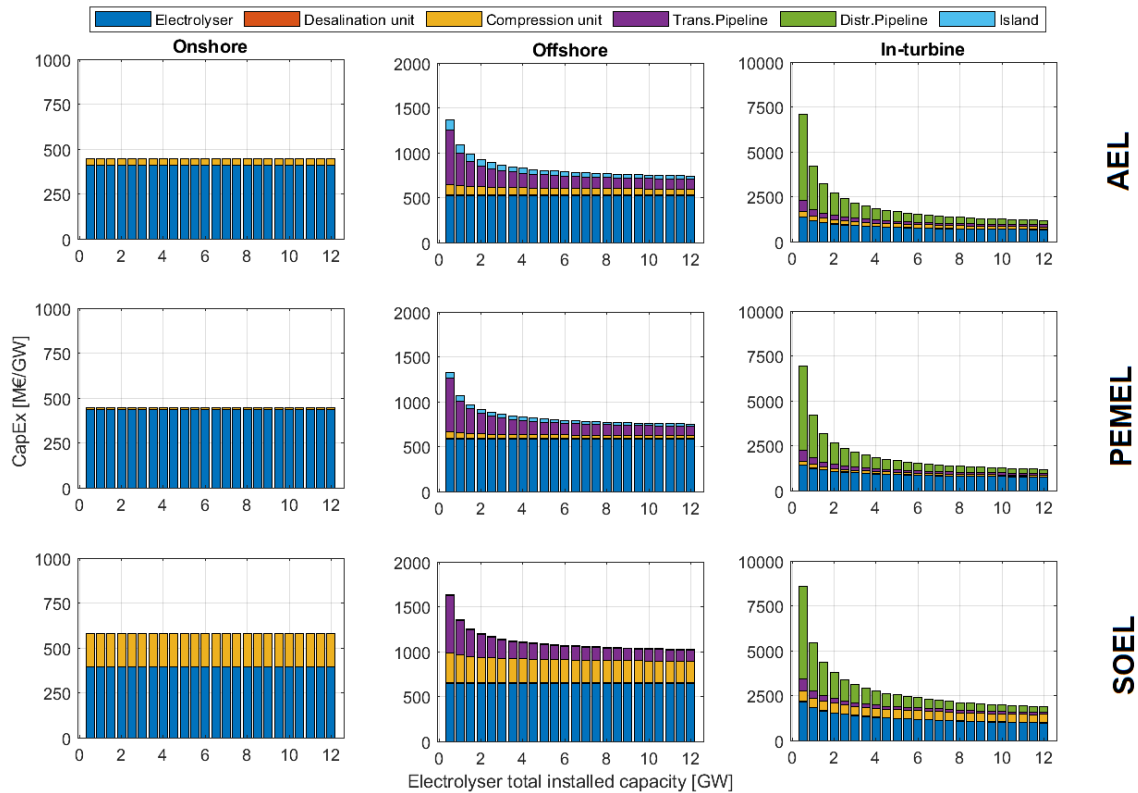


**Figure 5.** CapEx per unit of installed capacity. Note: these results are valid for both H<sub>2</sub>-driven and electricity-driven operation of the electrolyser.

### 1.5.1 H<sub>2</sub>-driven operation

OpEx per unit of installed capacity for the H<sub>2</sub> infrastructure is presented in **Figure 6**. The stack replacement is a major cost. The effect of the economies of scale is visible in the in-turbine case. Two stack replacements take place during the lifetime of the AEL and PEMEL electrolyser, and

four stack replacements are required for the SOEL electrolyser, due to the lower amount of maximum operating hours.

Purchasing tap water to the onshore electrolyser is a major cost.

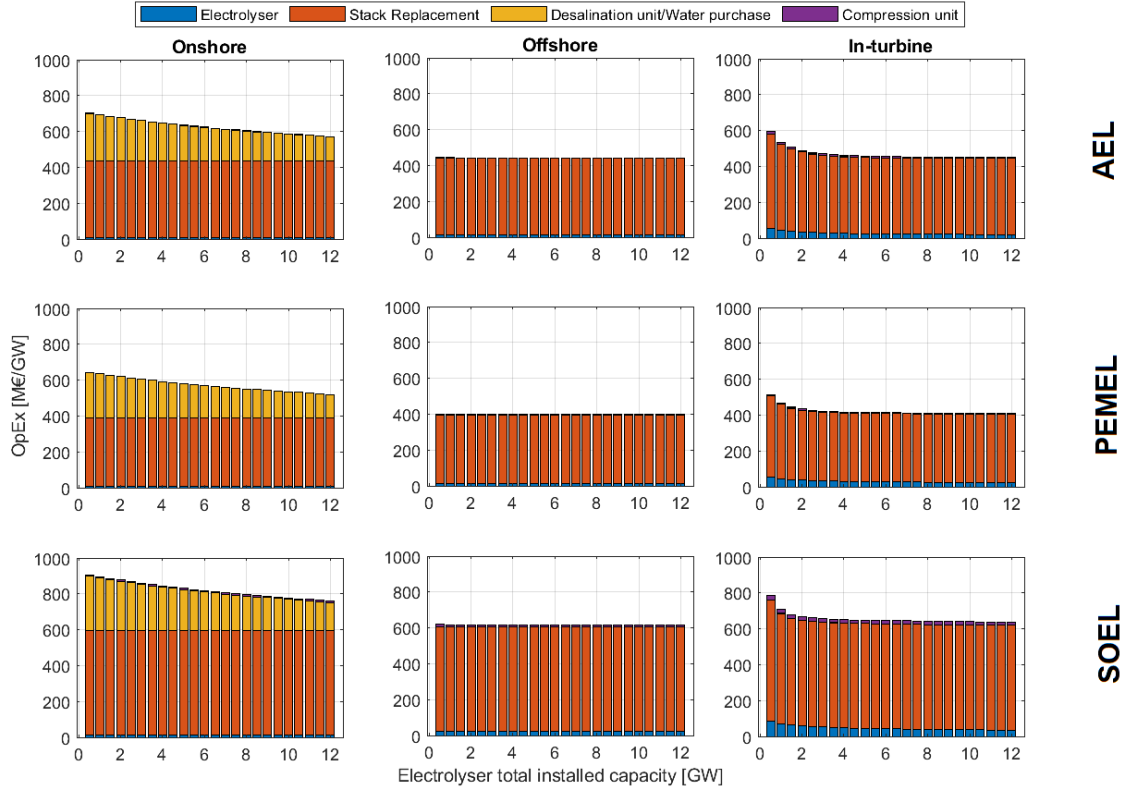


**Figure 6.** OpEx per unit of installed capacity, in the case of H<sub>2</sub>-driven operation.

The energy consumption and the energy delivered in form of H<sub>2</sub> per unit of installed capacity is presented in **Figure 7**. Both energy consumption and delivered decrease by increasing the installed capacity, due to lower capacity factors. AEL and PEMEL show similar performance. SOEL, although a better nominal efficiency, is penalised by slower cold start-up and by the higher stack degradation. Therefore, for a consumption identical to AEL and PEMEL, the energy delivered is less. Moreover, the consumption of the compressor for SOEL is higher than for AEL and PEMEL, because of a higher pressure ratio, thus reducing the electricity directed to the electrolyser.

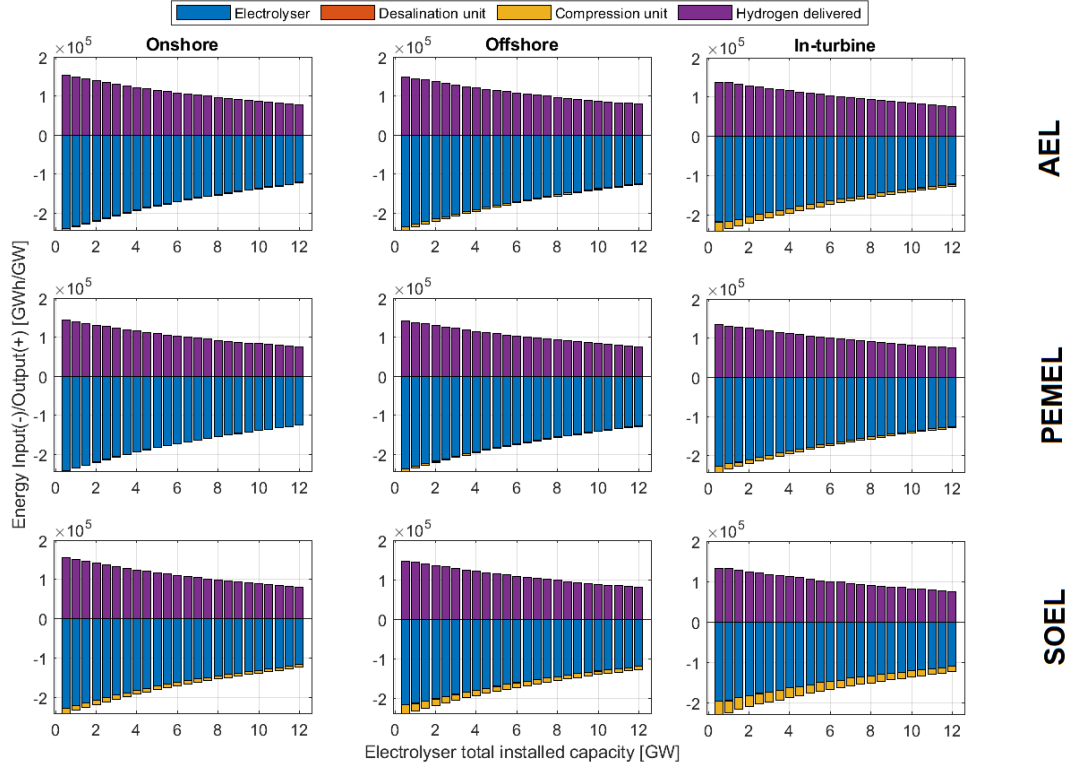


**Figure 7.** Energy consumed in form of electricity and delivered in form of  $H_2$ , in the case of  $H_2$ -driven operation.

The cost of purchasing electricity per unit of installed capacity is presented in **Figure 8**. This is an order of magnitude higher than the OpEx, resulting then to be the main cost driver, and also greater than the CapEx. The cost for the electricity purchased per unit of installed capacity decreases by increasing the installed capacity, due to the decreasing capacity factor. The cost for the purchased electricity is lower for the in-turbine placement, followed by the offshore and, finally, for the onshore placement. This is due to the cost of the electrical infrastructure upstream the electrolyser allocated in the cost of the electrical energy consumed by the  $H_2$  infrastructure, larger for the onshore placement, followed by the offshore and in-turbine placements.

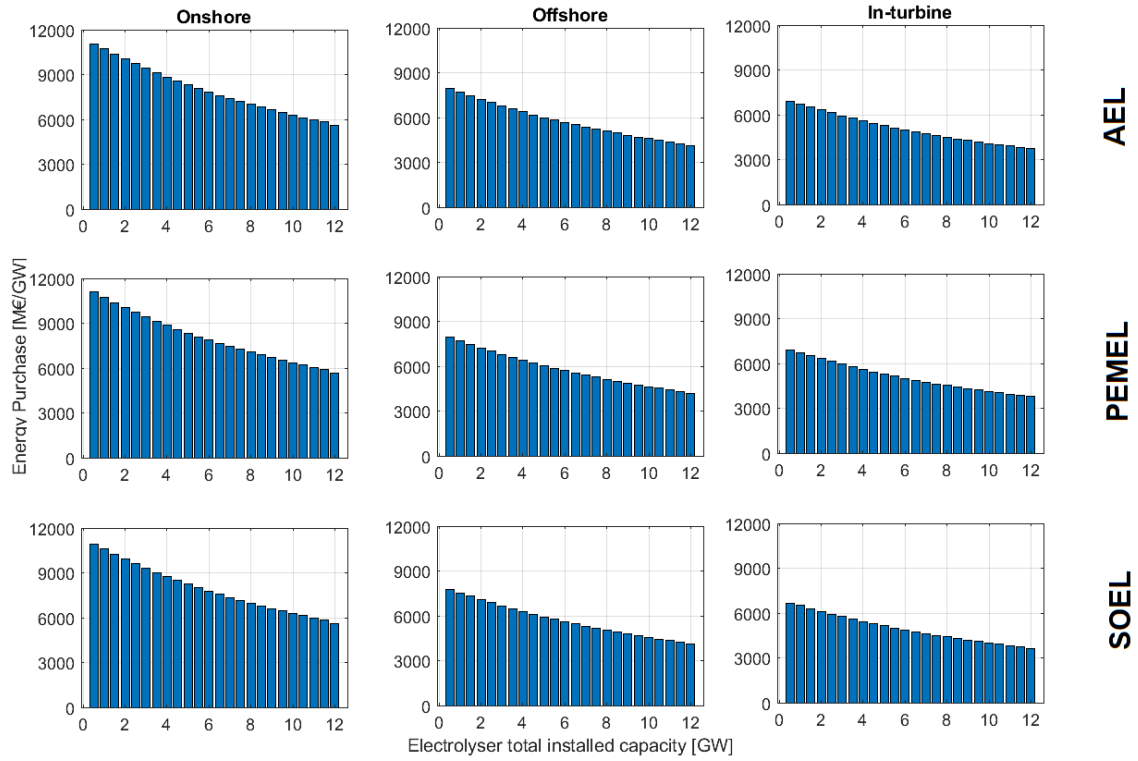


**Figure 8.** Electrical energy purchase per unit of installed capacity, in the case of H<sub>2</sub>-driven operation.

The final results of LCOH and LCOE for each electrolyser technology and placement are presented in **Figure 9**. The LCOH is the results of the interrelated effects of CapEx, OpEx, and electrical energy purchase and energy delivered. Lower LCOHs are found for AEL, even though very close to PEMEL. Higher CFs are found for PEMEL, due to lower electricity diverted to the compression unit compared to AEL and SOEL, due to a higher operating pressure of the PEMEL. The low operating pressure of the SOEL, 5 bar, largely penalises this technology for in-turbine applications. LCOE and CF of the power transmission to shore are independent of the electrolyser technology used. Therefore, the discussion regarding the electricity infrastructure in the case of AEL (in the Article) can be extended to PEMEL and SOEL.

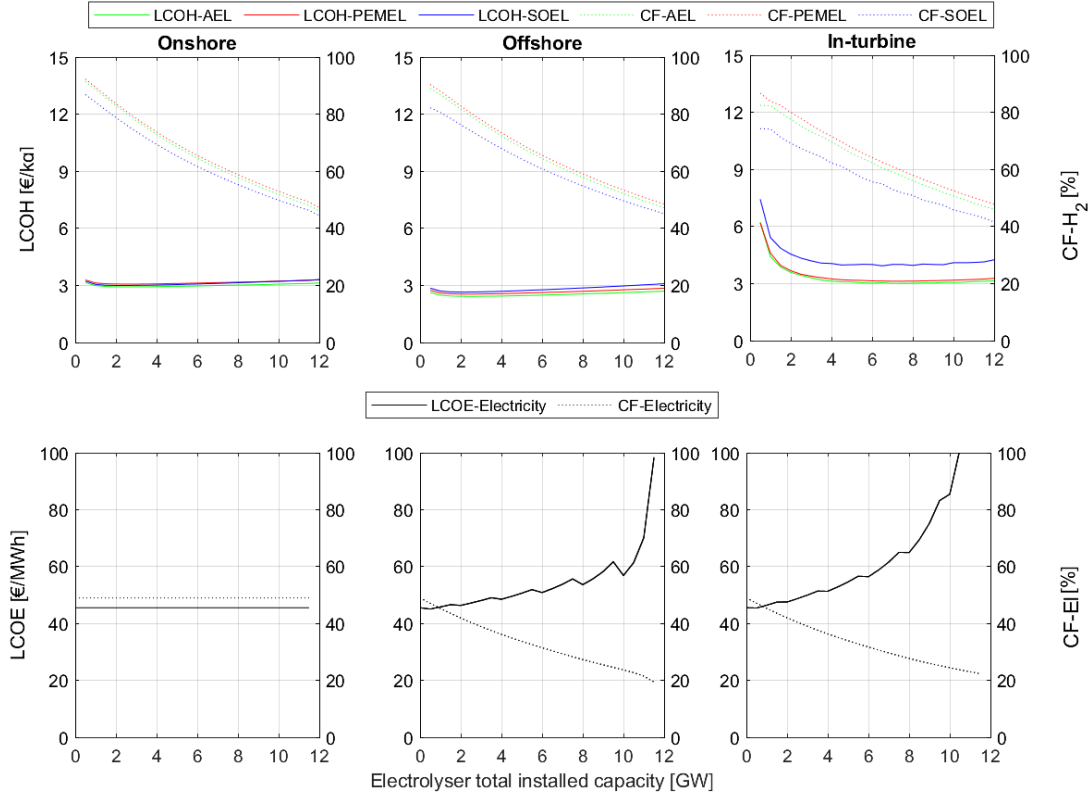


**Figure 9.** LCOH, LCOE and CF, in the case of H<sub>2</sub>-driven operation. CF-electricity is the capacity factor of the electricity infrastructure (e.g. HVDC transmission cable, HVDC converters, substations, etc.) from the Hub to shore.

### 1.5.2 Electricity-driven operation

OpEx per unit of installed capacity for the H<sub>2</sub> infrastructure is presented in **Figure 10**. Differently from the H<sub>2</sub>-driven operation, the stacks are not replaced for small sizes, due to operating hours lower than the maximum operating hours. The number of stack replacements increases with the electrolyser total installed capacity, due to the increasing CF (determining an increasing number of operational hours), up to two for AEL and PEMEL, and up to four for SOEL.

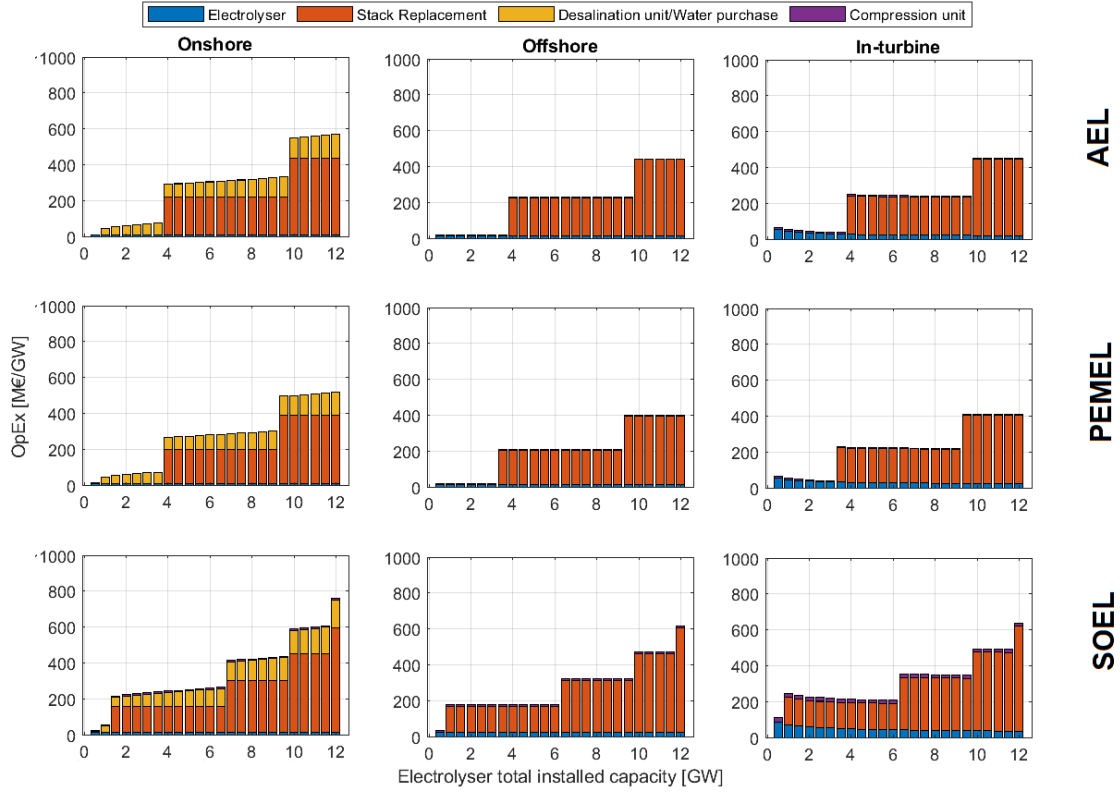


**Figure 10.** OpEx per unit of installed capacity, in the case of electricity-driven operation.

The energy consumption and the energy delivered in form of  $H_2$  per unit of installed capacity in **Figure 11**. Both energy consumption and delivered increases by increasing the scale, due to the increasing CFs. AEL and PEMEL show similar performance. SOEL is penalised by the slower cold start-up and by the higher degradation. Moreover, the consumption of the compressor for SOEL is higher than for AEL and PEMEL, because of the higher pressure ratio, therefore less electricity is converted to  $H_2$ . Due to the assumption for the electricity-driven operation that the priority is to cover the electrical demand onshore, all the losses in the electricity infrastructure upstream of the electrolyser are considered to be allocated in the part of electricity dedicated to the electrolyser. Therefore, the energy input decreases from the in-turbine to the onshore placement, due to the electric losses in the offshore electricity infrastructure. Due to the losses in the electricity infrastructure, in the onshore smallest case (i.e. assumed 500 MW in the model), no energy is consumed/generated by the AEL, and only an irrelevant portion in the PEMEL and SOEL, due to the wider load operational range.

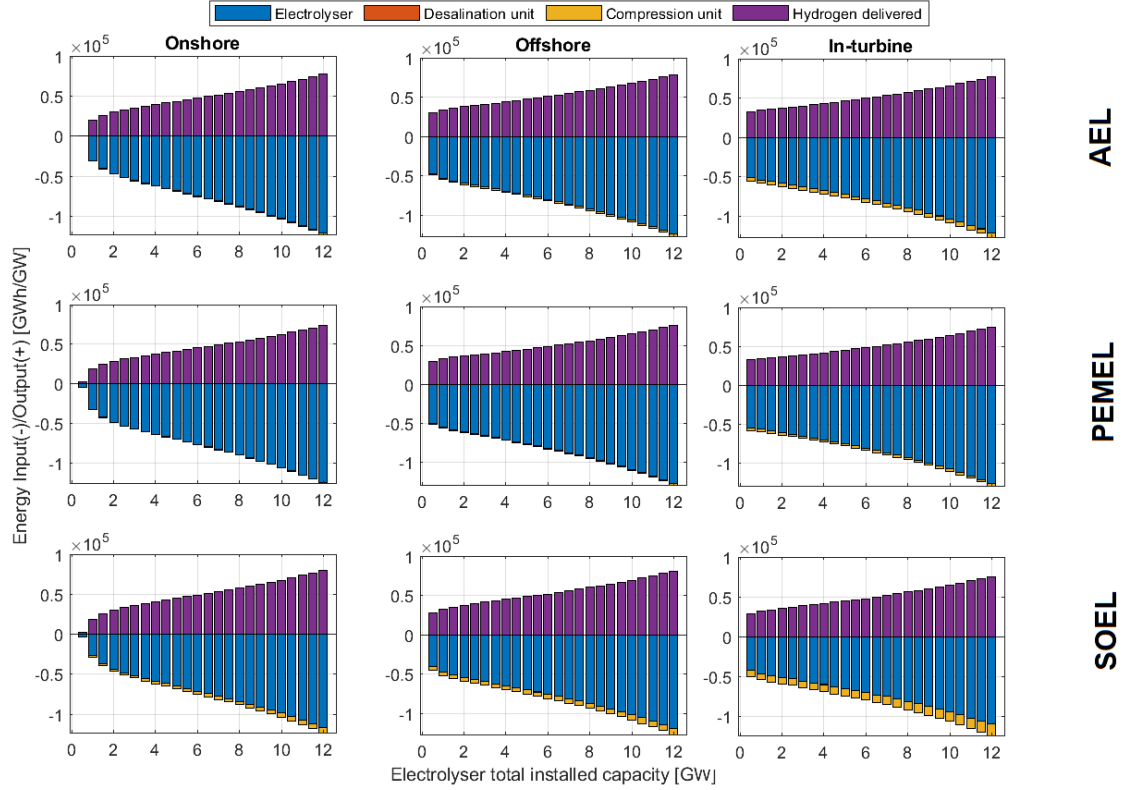


**Figure 11.** Energy consumed in form of electricity and delivered in form of H<sub>2</sub>, in the case of electricity-driven operation.

The cost of purchasing electricity per unit of installed capacity is presented in **Figure 12**. As in the case of H<sub>2</sub>-driven operation, this is an order of magnitude higher than the OpEx, and also greater than CapEx, resulting in the main cost driver. The cost for the purchased electricity per unit of installed capacity increases by increasing the installed capacity, due to the increasing CFs. As in the case of H<sub>2</sub>-driven operation, the cost for the purchased electricity is lower for the in-turbine placement, followed by the offshore and, finally, for the onshore placement. This is due to the cost of the electrical infrastructure upstream the electrolyser allocated in the cost of the electrical energy consumed by the H<sub>2</sub> infrastructure, larger for the onshore placement, followed by the offshore and in-turbine placements.

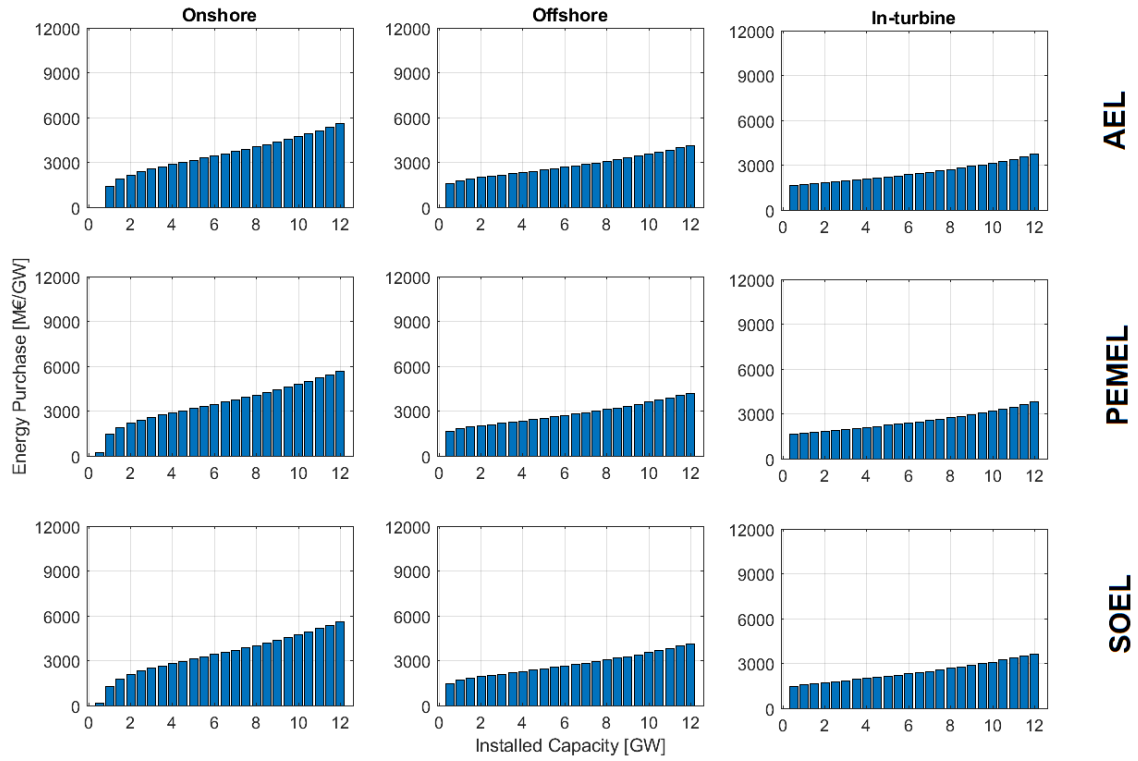


**Figure 12.** Electrical energy purchase per unit of capacity installed, in the case of electricity-driven operation.

The final results of LCOH and LCOE for each electrolyser technology and placement are presented in **Figure 13**. The LCOH is the results of the interrelated effects of CapEx, OpEx, and electrical energy purchase and energy delivered. Lower LCOHs are found for AEL, even though very close to PEMEL. The differences between the alternative technologies are due to the same reasons for the H<sub>2</sub>-driven operation (see the previous section). Moreover, we found that for central values of the electrolyser total installed capacity (i.e. from 2.5 GW to 6.5 GW) the LCOH of onshore SOEL is lower than the LCOE of offshore SOEL.

LCOE and CF of the power transmission to shore are independent of the electrolyser technology used. Therefore, the discussion regarding the electricity infrastructure in the case of AEL (in the Article) can be extended to PEMEL and SOEL.



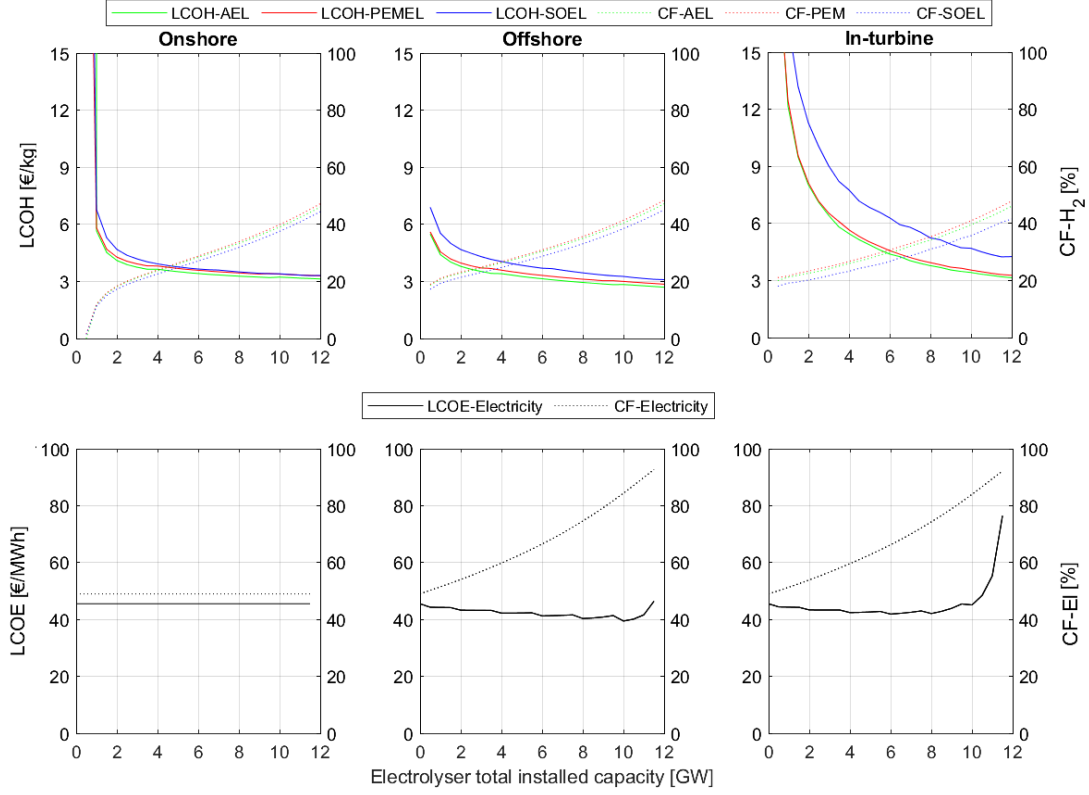


**Figure 13.** LCOH, LCOE and CF, in the case of electricity-driven operation. CF-electricity is the capacity factor of the electricity infrastructure (e.g. HVDC transmission cable, HVDC converters, substations, etc.) from the Hub to shore.

### 1.5.3 Sensitivity analysis

The effects on the median LCOH of each cost of each component is presented in **Figure 14** and **Figure 15**. The effects of the cost of each technology unit on LCOH already discussed for AEL in the main article are similar to PEMEL and SOEL, with a larger impact of the compression unit for the latter electrolyser type.

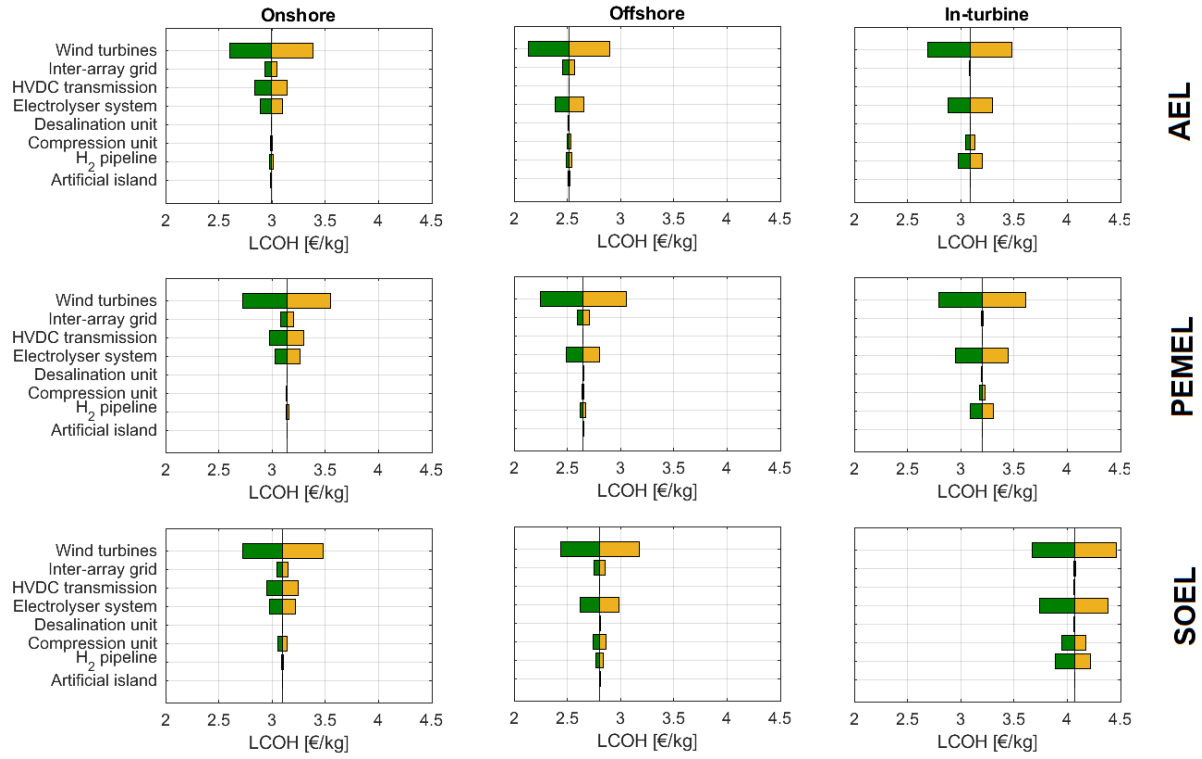


**Figure 14.** Median LCOH obtained by perturbation of +/-25% the CapEx of each component, in the case of H<sub>2</sub>-driven operation.

In the case of the electricity-driven operation (**Figure 15**), it is important to notice that the median value of LCOH for onshore SOEL is lower than the offshore value of LCOH for offshore SOEL.

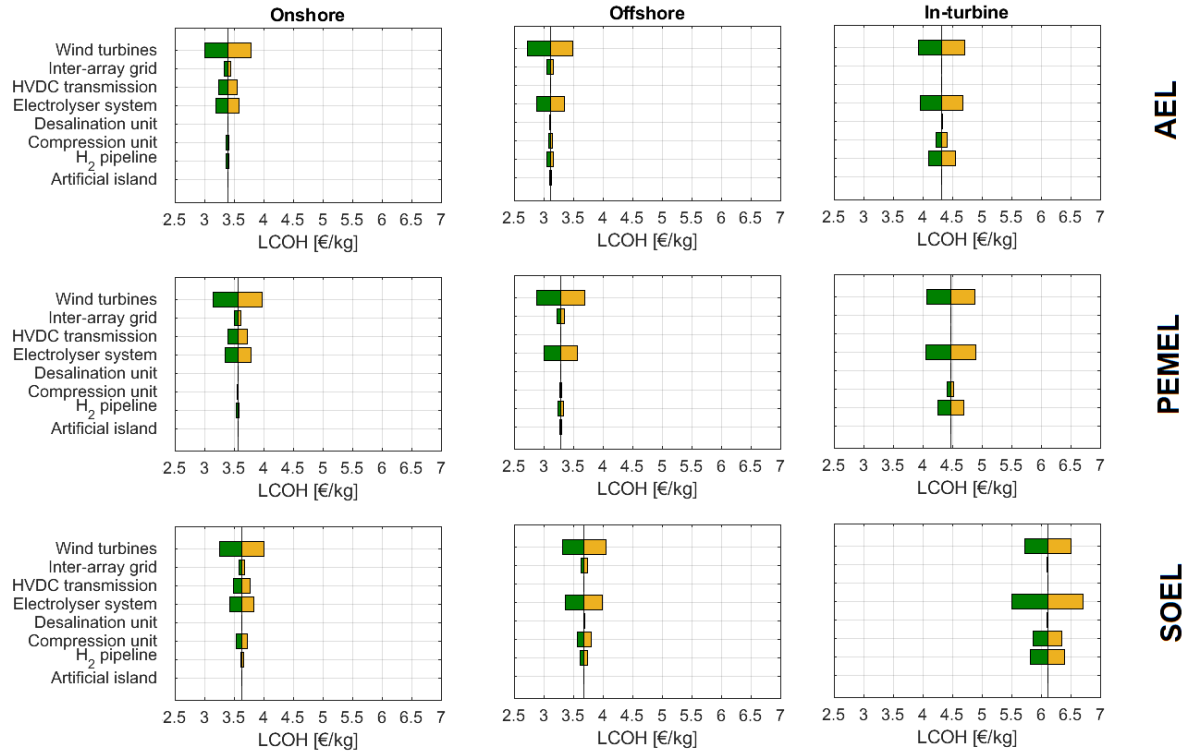


**Figure 15.** Median LCOH obtained by a perturbation of  $\pm 25\%$  the CapEx of each component, in the case of electricity-driven operation.

#### 1.5.4 Impact of the distance of the Hub

The relation between the LCOH and the distance of the Hub from the shore is presented in **Figure 16** and **Figure 17**. The effect of distance on LCOH already discussed for AEL in the main article are similar to PEMEL and SOEL, with higher costs for the in-turbine case of the latter technology, due to the additional compression required.

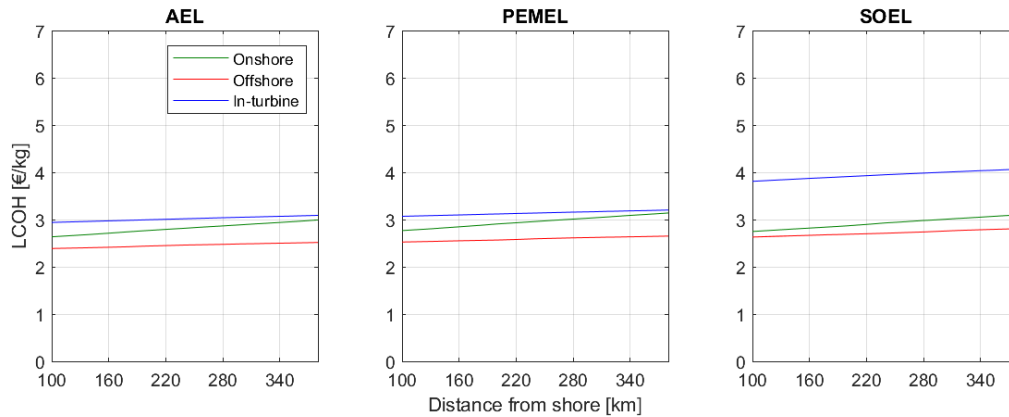


**Figure 16.** Median LCOH by the distance of the Hub to shore, in the case of H<sub>2</sub>-driven operation.

In the case of electricity-driven operation (**Figure 17**), the proximity to shore makes the onshore solution more competitive with the offshore solution. In the case of SOEL, the onshore placement is more cost-effective than the offshore placement.

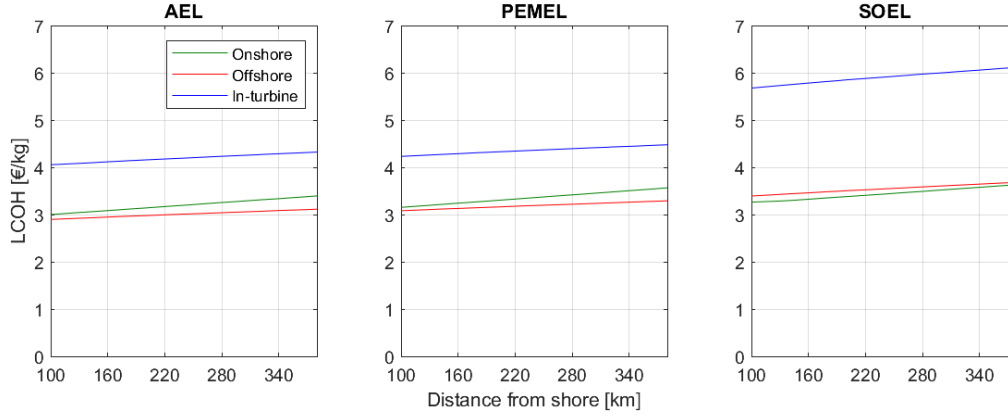


**Figure 17.** Median LCOH by the distance of the Hub to shore, in the case of electricity-driven operation.

### 1.5.5 Discussion on the footprint.

AEL is the technology with the largest footprint, occupying in the extreme case (i.e. 12 GW), 1.14 km<sup>2</sup>, in the case of the centralised offshore or offshore placement, or 1,425 m<sup>2</sup> in case of the in-turbine solution.

Considering a WT tower of 10 m of diameter<sup>3</sup>, the available horizontal area would be 78.5 m<sup>2</sup>. This would be enough to contain an AEL of 840 kW (without considering the desalination unit). The in-turbine design would be feasible with more compact designs of the electrolyser, otherwise, the electrolyser should be placed outside the WT.

## References

1. The MathWorks Inc. *MATLAB and Statistics Toolbox Release 2019b*. (2016).
2. Goodwin, D. G., Moffat, H. K. & Speth, R. L. *Cantera: An object- oriented software toolkit for chemical kinetics, thermodynamics, and transport processes*. (2017).
3. Gaertner, E. *et al.* *IEA Wind TCP Task 37: Definition of the IEA 15 MW Offshore Reference Wind Turbine*. (2020). doi:doi:10.2172/1603478
4. E.C.M. Ruijgrok PhD, E.J. van Druten MSc, B. H. B. Ms. *Cost Evaluation of North Sea Offshore Wind Post 2030*. (2019). doi:112522/19-001.830 112522
5. The Danish Energy Agency & Energinet. *Technology Data - Generation of Electricity and District heating*. 414 (2016).
6. Greedy & Lyndon. *TENNET, NL OFFSHORE WIND FARM TRANSMISSION SYSTEMS 66 kV Systems for Offshore Wind Farms*. 35 (2015).
7. U.S. Department of Energy. *Assessing HVDC Transmission for Impacts of Non - Dispatchable Generation*. 1–32 (2018).
8. Tractebel, E., Engie & Hincio. *Study on Early Business Cases for H2 in Energy Storage and More Broadly Power To H2 Applications*. *EU Comm*. 228 (2017).
9. IEA. *The Future of Hydrogen - Seizing today's opportunities*. *Rep. Prep. by IEA G20, Japan* (2019). doi:10.1787/1e0514c4-en
10. Renz, M., Schot, M. Van & Jepma, C. *North Sea Energy Energy transport and energy carriers*. (2020).
11. *Electricity Ten Year Statement 2015*. Appendix E: *Electricity Ten Year Statement*. 2015 (2015). doi:10.1016/B978-0-08-091906-5.00027-6
12. Swamy, S. K., Saraswati, N., Warnaar, P., Sea, N. & Power, W. *North Sea Wind Power Hub ( NSWPH ): Benefit study for ( 1 + 3 ) potential locations of an offshore hub- island ( Compressed Results )*. (2019). doi:06.37770
13. Jepma, C., Kok, G.-J., Renz, M., van Schot, M. & Wouters, K. *North Sea Energy D3.6 Towards sustainable energy production on the North Sea-Green hydrogen production and CO2 storage: onshore or offshore?* (2018).
14. ECMWF. *ERA5 hourly data on single levels from 1979 to present*. (2018). doi:10.24381/cds.adbb2d47
15. Danish Energy Agency and Energinet. *Technology Data for Renewable Fuels - Technology descriptions and projections for long-term energy system planning*. (2017).
16. Schmidt, O. *et al.* *Future cost and performance of water electrolysis: An expert elicitation study*. *Int. J. Hydrogen Energy* **42**, 30470–30492 (2017).
17. Bertuccioli, L. *et al.* *Development of water electrolysis in the European Union*. **23**, (2014).
18. Zauner, A., Böhm, H., Rosenfeld, D. C. & Tichler, R. *Innovative large-scale energy storage technologies and Power-to-Gas concepts after optimization*. D7.7 *Analysis on future*

- technology options and on techno-economic optimization. 1–89 (2019).
19. Menon, E. S. *Pipeline planning and construction field manual*. Gulf Professional Publishing is an imprint of Elsevier (Elsevier Inc., 2011).
  20. Weber, A. C. & Papageorgiou, L. G. Design of hydrogen transmission pipeline networks with hydraulics. *Chem. Eng. Res. Des.* **131**, 266–278 (2018).
  21. North Sea Wind Power Hub Consortium. *Modular Hub-and-Spoke Concept to Facilitate Large Scale Offshore Wind*. (2019).
  22. Lundberg, S. Performance comparison of wind park configurations. *Power Eng.* (2003).
  23. National Grid. Electricity Ten Year Statement 2015. *UK Electr. Transm.* 1–145 (2015).
  24. Siemens, Personal Communication on electrolyser offshore installation cost. (2020).
  25. CEER. Pan-European cost-efficiency benchmark for gas transmission system operators. (2019).
  26. Gerrits, S., Kuiper, C., Quist, P. & Van Druten, E. J. Feasibility Study of the Hub and Spoke Concept in the North Sea: Developing a Site Selection Model to Determine the Optimal Location. (Delft University of Technology, 2017).
  27. Das, K. & Antonios Cutululis, N. *Offshore Wind Power Plant Technology Catalogue - Components of wind power plants, AC collection systems and HVDC systems*. (2017).
  28. IRENA. *Hydrogen From Renewable Power: Technology outlook for the energy transition*. (2018).
  29. Reuß, M. *et al.* Seasonal storage and alternative carriers: A flexible hydrogen supply chain model. *Appl. Energy* **200**, 290–302 (2017).
  30. DANVA. *Water in figures*. (2019).